School of Industrial and Information Engineering

Master of Science Degree in Materials Engineering and Nanotechnology

POLITECNICO
MILANO 1863

Application of Carbon Nanotubes as adsorbent material for swimming pool water depuration

Supervisor: Prof. Carlo Spartaco Casari

Davide Delfrate
ID: 905484

Academic Year: 2020-2021

Before starting the argumentation of the thesis, I would like to thank the people who have been close and always supported me over these years, make it possible to achieve this goal.

I would like to say a big thank to my family, my grandparents nonna Laura and nonno Guido and nonni Luciano and Clara, my aunts and all my historical friends that always support me in my decisions. They made my time at University Politecnico di Milano easier and complete of experiences that I will bring with me for the entire life.

I would like to kiss my girlfriend Irene as she did every morning during these years spent as university student.

I would like to thank the team of Innovacarbon Srl that from the first time was very kind with me, in particular Danilo Vuono who helped me in the realization of the work and taught me a lot about the job and carbon nanotubes.

I remember the first day at Poli, lost in the stairs I met Migna, real travel companion, we have shared most of the classes and Acquario's study session.

Unforgettable the Erasmus community and parties with Ous, which allowed me to discover other cultures and open my mind.

I am sad to conclude this chapter of my life, but at the same time, I am very enthusiastic to the new one that wait me. I hope my efforts and the difficulties encountered at University will help me to be every day a better person.

Abstract

Carbon nanotubes (CNTs) are studied as adsorbent material for a lot of different substances, however, not so much industrial applications are reported.

The applicability of CNTs as adsorbent material for swimming pool water treatment is investigated in the present work.

Bathers can release in water contaminants directly or indirectly, the interaction of these substances with chlorine can lead to formation of disinfection by-products (DBPs) such as trihalomethanes (THMs) and haloacetic acids (HAAs). Studies have demonstrated the correlation between bladder cancer and prolonged contact with these contaminants.

The aim of this study is to verify if CNTs could be promising material to substitute the commercial swimming pool filter materials, who have some limitation.

CNTs used are synthesized by cvd technique, in situ by Innovacarbon srl and are directly supported on quartz sand.

The adsorption behaviour of the material is tested for three typical contaminants of swimming pool water: ammonia, urea and solar oil. Possible mechanism of adsorption of carbon nanotubes are investigated through the application of kinetics and equilibrium isotherm models to experimental data obtained from treatment of the polluted water.

A state of art of swimming pool filters and an overview of CNTs and adsorption mechanism is also present.

The material has given a great respond for what concern solar oil with a maximum adsorption capacity of about 2500 $mg_{solar\ oil}/g_{CNTs}$, while for urea and ammonia the values of maximum adsorption capacity are below the expectation, with respectively 3,6 mg_{urea}/g_{CNTs} and 0,56 mg_{NH_3}/g_{CNTs}.

Keywords Carbon nanotubes; Adsorption; Swimming pool; Water filters.

Riassunto

I nanotubi di carbonio (CNTs) sono studiati come materiale adsorbente per diversi tipi di sostanze, le applicazioni industriali sono però limitate.

Nel presente lavoro viene studiata l'applicabilità dei CNTs come materiale adsorbente per il trattamento delle acque delle piscine.

I bagnanti possono rilasciare direttamente o indirettamente contaminanti nell'acqua, l'interazione di queste sostanze con il cloro disinfettante può portare alla formazione di sottoprodotti di disinfezione (DBP) come trialometani (THMs) e acidi aloacetici (HAAs). Diversi studi hanno dimostrato una correlazione tra cancro alla vescica e contatto prolungato con questi contaminanti.

Lo scopo di questo studio è verificare se i CNTs potrebbero essere promettenti per sostituire i materiali filtranti per piscine comunemente utilizzati, che presentano varie limitazioni.

I CNTs utilizzati sono sintetizzati con tecnica cvd, in situ da Innovacarbon srl e sono direttamente supportati su sabbia di quarzo.

Il comportamento di adsorbimento del materiale è testato su tre tipici contaminanti delle piscine: ammoniaca, urea e olio solare. I possibili meccanismi di adsorbimento dei CNTs sono studiati attraverso l'applicazione di modelli cinetici e isoterme di equilibrio a dati sperimentali ottenuti dal trattamento dell'acqua inquinata.

È presente anche uno stato dell'arte dei filtri per piscine e una panoramica sui CNTs e sui meccanismi di adsorbimento.

Il materiale ha dato un ottimo riscontro per l'adsorbimento di olio solare con una capacità massima di adsorbimento di circa 2500 $mg_{solar\ oil}/g_{CNTs}$, mentre per urea e ammoniaca i valori di capacità massima di adsorbimento sono inferiori alle aspettative, con rispettivamente 3,6 mg_{urea}/ g_{CNT} e 0,56 mg_{NH_3} / g_{CNT}.

Keywords Nanotubi di carbonio; Adsorbimento; Piscina; Trattamento acque.

Table of contents

Introduction

Water, essential element for life on earth. The availability of water is every day more and more at risk, due to climate change, the supply of clean water is already a great problem and will be even greater in future. For this reason, it is of primary importance, avoid as much as possible waste of this fundamental resource and when possible, recover it.

Industries, many times, underestimate and make it only an economic issue, the risk of spillage of polluted waters in natural systems. Anyway, an ever increasing number of companies and researchers invest their time and funds to seek always better and more efficient adsorbent materials and technology solutions to this problem. Although great amount of work has been reported on the performance of carbonaceous materials, in particular CNT/graphene-based nanomaterials in treatment of wastewater, engineering challenges still exist for their practical application.

During pool activities, humans introduce directly or indirectly substances such as skin particles, sweat, urine, faecal, and hair and personal care products as sunscreen, body lotion, shampoos, and other cosmetics in the water of the pool. The risk to be exposed to chemicals substances, viruses and bacteria during swimming pool activities has been reported several times. Cases of bladder cancer and respiratory issues are not irrelevant and some diseases or symptoms such as gastroenteritis and dermatitis are still more frequents if filtration system does not work perfectly.

In this work will be studied the applicability of carbon nanotubes created by Innovacarbon SRL as a new filter material for swimming pool, to this purpose will be test the adsorption behaviour of the material with three substances frequently present in swimming pool: ammonia, urea and solar oil. The material has already demonstrated great absorption stats compared to other adsorbent materials, for organic wastewater, reactive dyes, hydrocarbons, aromatic compounds, polyphenol and more. But this application has never been studied.

The objective is to try to eliminate these substances from the pool, to avoid the side reaction of the chlorine with ammoniacal and organic substances. The adsorption mechanisms and possible interactions between carbon nanotubes and these substances will be studied through kinetic experiments and equilibrium isotherms studies.

1 Swimming pool issues and state of art of the filters

Across the world, Swimming is a year by year increasing activity for entertainment and exercise. This popularity brings with itself an increasing of the related troubles.

The number of research that focus on possible relations between swimming pool activities and diseases or symptoms such as gastroenteritis and dermatitis or bladder cancer have increased exponentially in the last years. [1]

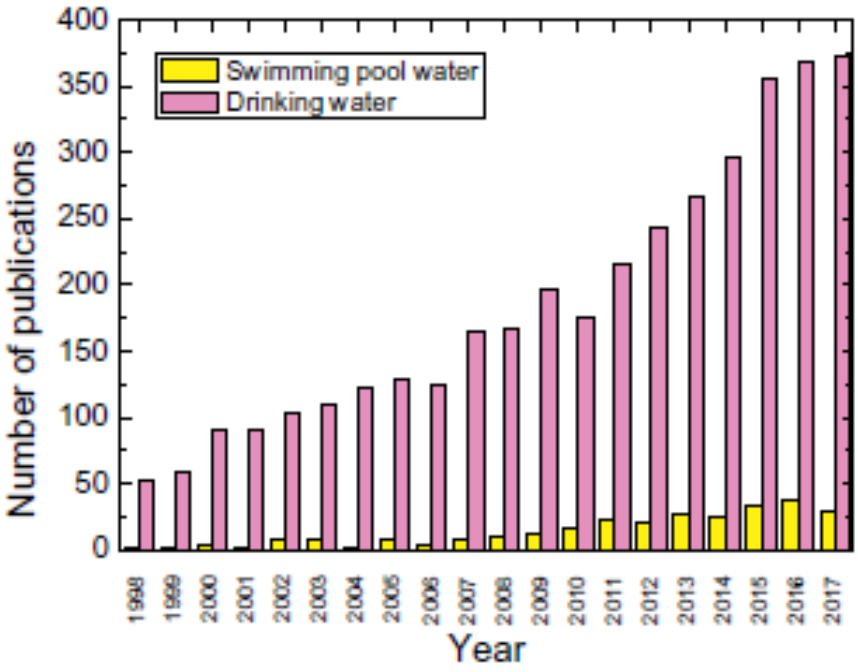

Figure 1: Number of publications in relation with Disinfectant By Products in Swimming Pool Waters and Drinking Waters in the period (1998-2017).

The direct consequence is a constant growing of the demand of filters, and the needed of better materials and technologies is not secondary.

1.1 Contaminants

During pool activities, human substances such as skin particles, sweat, urine, faecal, and hair and personal care products as sunscreen, body lotion, shampoos, and other cosmetics could contaminate the water of the pool. The chemistry of

the pool water is transformed by these materials, collectively called “body fluids.”

Additional pollutants for outdoor pools come from the surrounding environment or from the rainwater that can bring leaves and dust. The presence of suspended solids and any particulate matter may increase the resistance of most microbes to disinfection because the particles act as shields for the virus and bacteria.

These contaminants may carry pathogens, including viruses, protozoa (Giardia and Cryptosporidium), and bacteria such as Shigella and Escherichia coli that can lead to some diseases or symptoms such as gastroenteritis and dermatitis. [1]

There are three main ways of exposure to chemicals in swimming pools and similar environments: direct ingestion of the water, inhalation of volatile and dermal contact with absorption through the skin.

The majority of the organic pollutant and contaminants is concentrated at or near the surface of the pool, irrespective of the mixing effects of the circulation system.

With respect to indoor pools, outdoor pools have a natural ventilation that increase volatilisation of chemicals contaminants, reducing the residual level of pollutants also thanks to sunlight photolysis [2].

In a critical review of Bradford is estimate that one bather in one hour of normal swimming exudes 0.494 g of reduced nitrogen (NH_3–N and organic-N compounds), 0.410 g of organic-N, mostly (0.345 g) as urea and (0.084 g) NH_3–N and 0.287 g of total organic carbon (TOC). All these contaminants, including inorganic salts are classified as total dissolved solids (TDS). As the concentration of these contaminants increase, the disinfectant dose (usually chlorine or bromine) required to maintain an acceptable free available chlorine (FAC) and/or total chlorine (TC) concentration for public safety purposes also increases. [3]

With the aim to avoid the spread of infections and diseases, the priority of the disinfection process is to maintain adequate microbial water quality.

Viruses and bacteria in swimming pool are controlled by treatment based on filtration, flocculation and the adequate application of chlorine and other disinfectants, anyway the recirculation of the water in the swimming pool can lead to an accumulation of different chemical contaminants who cannot be

adsorbed by the filter and so to a situation in which water quality standard are not satisfactory.

Sometimes may occurs interaction between the disinfectants and the pollutants, bringing to the formation of new chemicals compound named as disinfectant by-product (DBP), increasing attention is given to the potential significance of exposure to these chemicals by bathers. [4]

Trihalomethanes (THMs) and halo acetic acids (HAAs) are the principal DBPs encountered in swimming pool water, it has been found a correlation between ingestion of water contaminated by these pollutants and bladder cancer. [5]

Country	THMs (μg/L)					Pool type[a]
	$CHCl_3$	$CHCl_2Br$	$CHClBr_2$	$CHBr_3$	THMs	
U.S.	71 (25–207)	4 (1–28)	4 (1 – 10)	< 1	80 (26–213)	23 indoor (Cl)
	~25	< LOD	~2	< LOD		1 indoor (Cl)
	63 (16–138)		6 (1–35)	7 (1–55)	78 (19–146)	11 indoor (Cl)
	80–130					4 indoor (Cl)
	70–140					2 outdoor (Cl)
	81 (12–282)		2 (N.D.–10)	1 (N.D.–32)	77 (33–282)	1 indoor (Cl)
Canada					44 (18–114)	15 indoor (Cl)
					98 (12 – 311)	39 outdoor (Cl)
	18–80					8 indoor (–)
	29 (13–46)				29 (13–46)	2 indoor (Cl)
Germany					39 (5–125)	2 outdoor (TCCA)
					21	1 indoor (Cl)
					35–47	2 outdoor (Cl)
	18 (7–25)					1 indoor (Cl)
	23 (21–27)	3 (2–3)	< 0.5	< 0.4	27 (25–30)	3 indoor (–)
	3–28	0.7–6	0.03–7	0.02–0.8		Indoor (–)
					14 (6–43)	Indoor (–)
Spain	15 (8–21)	14 (9–27)	13 (7–23)	7 (3–17)	50 (35–75)	1 indoor (Cl)
	< 0.3	< 0.7	2 (2–3)	57 (52–64)	60 (54–67)	1 indoor (BCDMH)
	13.7 ± 7.3	1.4 ± 0.7	0. 5 ± 0.5	0.3 ± 0.7	15.8 ± 7.2	20 indoor (–)
					45.4 ± 7.3	1 indoor (Cl)
	15 (9–20)	14 (9–25)	13 (7–23)	7 (3–16)	50	1 indoor (Cl)
	< 0.3	< 0.6	2 (2–3)	60 (52–61)	63	1 indoor (BCDMH)
France	< 0.3	0.3 (0.1–1.1)	19 (3–64)	300 (29–931)	320 (32–996)	8 indoor (seawater)
	67 (47–82)	9 (5–12)	3 (1–5)	1 (1–2)	80 (64–98)	3 indoor (Cl)
	70	8	2	0.6	80	1 outdoor (Cl)
	N.D.	N.D.	4 (2–5)	66 (49–87)	70 (50–92)	3 indoor (seawater)
Australia	76 (65–84)	2 (2–3)	0.3–0.4	< 0.1	79 (67–87)	1 outdoor (Cl)
Italy	33.2 ± 24.6	4.2 ± 1.3	1.9 ± 2.0	0.4 ± 0.5	39.8 ± 21.7	5 indoor (Cl)
Ireland	88–116	17–18			105–133	3 indoor (Cl)
England	121 (45–212)	8 (3 – 23)	3 (1–7)	1 (1–2)	132 (57–223)	8 indoor (Cl)
Korea	21 (N.D.–46)	2 (N.D.–7)	N.D.	N.D.	23	86 indoor (three disinfectants)
Singapore	74 (30–167)	4 (1 – 12)	< 1	< 0.5	90 (32–170)	9 outdoor (–)

Table 1: THM concentration in swimming pool in different countries [1]

In addition, chronic exposure to these substances has been related to the development of respiratory tract irritations and asthma. [6]

The water quality can be tested by the measurement of turbidity, it is the cloudiness of a fluid caused by large numbers of individual particles that are generally invisible to the naked eye. Turbidity is measured in nephelometric

turbidity units (NTU), ISO 7027 provides the method for the determination of turbidity.

The maximum allowable turbidity for drinking water is 4 NTU, although municipal supplies should normally achieve <0.5 NTU prior to disinfection. For pool water, the turbidity should be <0.5 NTU, which is almost an order of magnitude lower than the limit of detection by the naked eye. [7] [8]

Chlorine

Chlorination is the most commonly used disinfection approach for swimming pool water treatment, it kills bacteria by attacking their lipids in the cell walls and destroying the enzymes and structures inside the cell. [9]

The WHO health-based guideline value for chlorine in drinking-water is 5 mg/l, for swimming pools, every country has its own normative but generally the concentration must be below 3-5 mg/L. [10]

Chlorine based disinfectants mainly include chlorine gas (Cl_2), sodium hypochlorite (NaClO), chlorinated isocyanurates and calcium hypochlorite ($Ca(ClO)_2$).

The hydrolysis and/or dissociation of these disinfectants produce hypochlorous acid (HClO) and hypochlorite ion (ClO^-) as active ingredients for disinfection.

The equilibrium between HClO and ClO^- is pH and temperature dependent.

$$Cl_2 + H_2O \rightarrow HClO + H^+ + Cl^-$$

The summation of HClO and ClO^- (active ingredients for disinfection) is defined as free available chlorine (FAC). The quantity control of free chlorine in swimming pool water is essential, its excess may cause problems to swimmers such as skin irritation while its insufficiency weakens microbial killing.

The chlorinous odours are the result of reactions between FAC and inorganic (NH_3–N) and organic nitrogen (organic-N) to form volatile chloramines, primarily dichloramine ($NHCl_2$) and trichloramine (NCl_3).

Trihalomethanes (THMs; $CHCl_3$, $CHBrCl_2$, $CHBr_2Cl$ and $CHBr_3$) are the more dangerous DBPs formed during the chlorination of water. About the limits of concentration of these molecules in water, every country has its own rules, U.S. EPA constrained the presence of THMs with a maximum contaminant level of 80 parts per billion (80 µg/l). [11]

Ammonia

Ammonia is a compound of nitrogen and hydrogen with formula NH_3, in the United States and in many more states it is classified as an extremely hazardous substance.

Its molar mass is of 17,031 g/mol, it appears as colourless gas due to its boiling point at -33°C, so it is usually found dissolved in water.

Ammonia can be released in water accidentally by the bathers through urine or sweat, as it is a very tiny molecule, it is difficult to be adsorbed with conventional swimming pool filters so tends to remain dissolved in water. Anyway, its concentration in swimming pool does not reach values greater than some µg/l.

Nitrogen compounds are not the direct cause of risk but can react with free disinfectant such as chlorine and bromine, extremely rapidly, to produce several by-products as chloramines.

Urea

Urea is a chemical compound with formula $CO(NH_2)_2$ and molar mass equal to 60,06 g/mol, in standard condition it appears as white crystalline solid.

Human body fluids are released from swimmers during pool activities, urine and sweat are two main sources of contaminants produced. Urea is a natural product of nitrogen and protein metabolism and an abundant component of urine. The mean content of urea and ammonia in urine is 10 240 mg/l and 560 mg/l, respectively, but hydrolysis of urea will give rise to more ammonia in the water. [10]

If found in swimming pool waters at high concentrations, can react with free chlorine to form chloramine, which may lead to eye and upper respiratory tract irritation and development of Asthma. [12]

Solar oil

The presence of oily substances in swimming pool is typical of outdoor pool, the carelessness of the bathers can bring a lot of body products, such as solar oil, solar cream, body lotion, shampoo and many more inside the pool.

Due to a density usually inferior to the water one, they can be found especially on the surface, giving an unpleasant appearance at the water.

The highly hydrophobicity promotes adhesion of these substances to the swimming pool wall, making them difficult to be remove without the use of specific cleaner instruments.

1.2 Swimming pool filters

Traditionally, the aim of filtration is to clarify the water removing suspended solids to ensure that lifeguards can see across the whole of the bottom of the pool.

With the pass of the year more attention was given to eliminate not only turbidity, but also DBP and bacteria.

1.2.1 Filters working principles

The water treatment process of swimming pools typically includes a combination of filtration to physically remove particles from the water and disinfection by maintaining a residual concentration of an appropriate biocide in the pool water to kill or inhibit the growth of microorganisms.

If the particles to be removed are too tiny or too much turbidity is present, the filtration step can be preceded by coagulation and clarification processes, also flocculation can be adopted to form bigger aggregates of pollutants, they can form clusters that are more easily transported and deposited on the filter medium.

Turnover time is a valid indicator to assess if water recirculation is adequate to maintain a good water quality. This is considered as the time necessary by a volume of water equivalent to the volume of the pool to pass through the filtration and circulation system. It is calculated from the ratio of the volume of water in the pool to the circulation rate (conventionally expressed in hours).

An effective filtration system including coagulation must remove more than 90% of *Cryptosporidium* oocysts in a single pass of water through the filter bed.

Every swimming pool could present a different situation depending on mixing efficiency, more turnover could be required to treat at least once the entire volume of water. Theory indicates that only 63% of the water in the pool will pass through the filtration system in one turnover time, even if the water in the pool is perfectly mixed at all times. After six turnovers, the amount of untreated water remaining in the pool will be equivalent to 0.25% of the water originally present in the pool. [8]

PWTAG code of practice gives an indication about turnover period for different type of pool, some examples are reported: [8]

- 3-4 h Competition pools 50m long.
- 4-8 h diving pools.
- 4-8 h domestic pools.
- 30-90 min hydrotherapy pools

Transport of particles in aqueous solutions during filtration occurs with a laminar flow and can involves multiple mechanisms depending upon the particle size:

- straining, if the particle size is larger than the void size
- sedimentation and interception, for particle above 1 µm but smaller than the void size
- diffusion, for particle size below 1 µm.

The filtration process consists of a transport stage, which takes particles closer to the filter media and an attachment stage that depends upon particle-surface interactions. Detachment is considered to be an additional stage as well, causing particles to re-join the flow, an increase in flow rate can enhance this side effect, especially for particles that are less strongly linked. [13]

While transport is mainly a physical step, attachment is mostly chemical, it is a consequence of short-range surface forces.

The filtration process can be driven by gravitational force (rapid gravity filtration), or by pressure (pressure filtration).

Additionally, filtration can be classified in terms of continuous or semi-continuous operation, the latter being the case when the filter has to be put offline to be backwashed. This is the case of the filters used in the present work.

When the filter has saturated, in order to clean it, the backwash is performed by inverting clean water so that the filter is flushed, usually 2.5 times the bed volume of water is used.

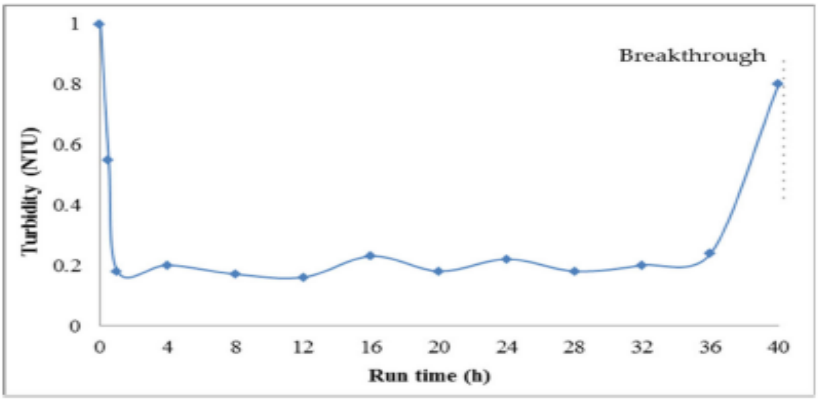

Figure 2: Turbidity as a function of run time for a typical filter run.

1.2.2 Sand filters

Sand filters are nowadays the most employed filters for swimming pools.

The filtration efficiency is determined by physical characteristics, such as grain size, shape, porosity and bed depth/media grain size ratio.

A swimming pool sand filter bed consists of packed solid particles, average density of about 1500 kg/m^3, ranging in size from 0.4 mm to 1.2 mm, with the majority normally being in the range 500–800 µm.

The spaces between the packed sand particles (the porosity) make up 35–50% of the total volume occupied by the particles, depending on how rounded or irregular is the shape of the grains.

Therefore, the smallest pore size will be of about 0.1 mm (100 µm), so particles smaller than this (more or less the smallest size that can be resolved by the naked eye) will not be removed by a simple straining mechanism but will move into the body of the media bed rather than being retained at the surface. However, as larger particles become trapped within the pores, the space sizes are reduced further, and smaller particles can be retained.

As water travels through the pores between the sand particles, it will pass by the extensive surfaces of the sand grains. For example, 1 m^3 volume of 0.6 mm diameter spheres will have an estimated total surface area of 6,252 m^2. [7]

Particles which are too small to be screened could be retained by the filter media as a result of weak intermolecular binding forces coming into play if the particles can get very close (within nanometres) to the surface of the sand grains.

The flow rate will not affect the removal of particles >100 µm in size. However, the efficiency in removing particles <100 µm in size, where the mechanism of removal depends on sedimentation, impaction and Brownian motion will decrease with an increase of the flow rate. [7]

Based on sand filtration rates, the flow rate can be classified in three categories:

- low-rate up to 10 m/h
- medium-rate 10 to 25 m/h
- high-rate 25 to 50 m/h

However, the maximum recommended surface water velocity through the filter in public pools with medium-rate filters is $25\ m/h$. In general, the faster the rate of flow of water through the filter the lower the filtration efficiency. [7] [8]

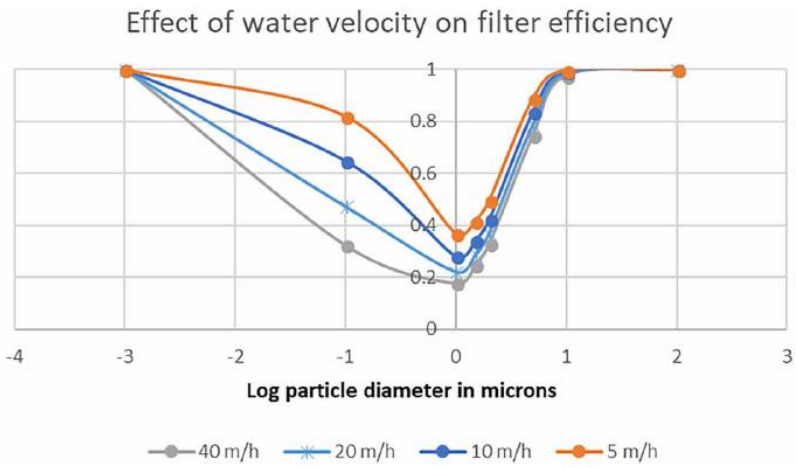

Figure 3: Effect of water velocity on filter efficiency, varying the particle diameter.

One approach to quantifying the effectiveness of particle removal by filters is to compare the measurements of the particle contents of the influent and effluent. The simplest index of the effectiveness of filtration is the filter efficiency (E), defined as the fraction (often expressed as a percentage) of particles removed from water as it passes through the filter:

$$E = \frac{C_0 - C_L}{C_0}$$

where C_0 and C_L are the influent and effluent solid concentrations (or the particle counts, or turbidity, depending on the measurements made).

However, E is not just a measure of the effectiveness of the media in removing particles, as this depends also on the depth of the media bed.

Considering the bed to be composed of uniform spheres acting as collectors, the removal at any given plane at a certain distance from the surface of the media will be a function of the number of collectors located within that distance. This gives rise to an exponential decrease in the particle content as water moves down through the filter:

$$C_L = C_0\, exp(-\lambda L)$$

Where $\mathrm{L}\ (\mathrm{m})$ is the filter depth and λ is the filter coefficient. 1/λ (m) is known as the characteristic length of the filter, which is sometimes used as a measure of the intrinsic effectiveness of the media in removing particles. For single-grade filters the sand bed should be a minimum of 800 mm deep. [13]

Moreover, media with a large grain diameter have to be employed in order to decrease the head loss. It is also possible to coupling different materials together to increase the filter efficiency as single sand medium filters cannot always perform adequately to achieve the treatment tasks. A solution was found in the introduction of dual media filters by placing a denser material at the bottom and a lighter one at the top, with decreasing size. for multi-grade filters the sand bed should be a minimum 550mm deep supported on a bed of coarser material 250mm deep.

Figure 4: Multilayer filter.

In the most common configuration, a layer of anthracite is placed on top of a sand layer and in some cases, an additional layer of garnet is added.

Anyway, sand filters show some limits, in particular low efficiency in removing organic material, for this reason other materials have been proposed and investigated as alternative.

1.2.3 Alternative filter's material

The research of new filter materials is an hot topic for what concern the water treatment and the reducing of environmental risk derived by the unconscious disposal of substances in aquatic environment.

Activated carbon is one of the most used material nowadays for water filtration due to its low cost compared to its adsorption capacity, arising from their large surface area and porosity. Two types of carbon are most often used for water filtration: powdered activated carbon (PAC) and granular activated carbon (GAC)

Physical adsorption is the main way in which activated carbon filters out a given substance. As liquid or air comes into contact with activated carbon, intermolecular forces draw molecules into the millions of pores and pockets on the surface of activated carbon. Beyond physical adsorption, activated carbon also facilitates chemical reactions, for example when chlorine comes into contact with activated carbon, both molecules react to form chloride ions, effectively removing chlorine from water, really, in an application as swimming pool filter this could be a drawback. Also, typical household water filtration units take advantage of this adsorbing agent for the removal of metal ions.

However, the poor reusability of activated carbon derived from the difficulty and the high cost to clean it and its limited capacity to uptake larger molecules due to size exclusion effects, are limitation for applications.

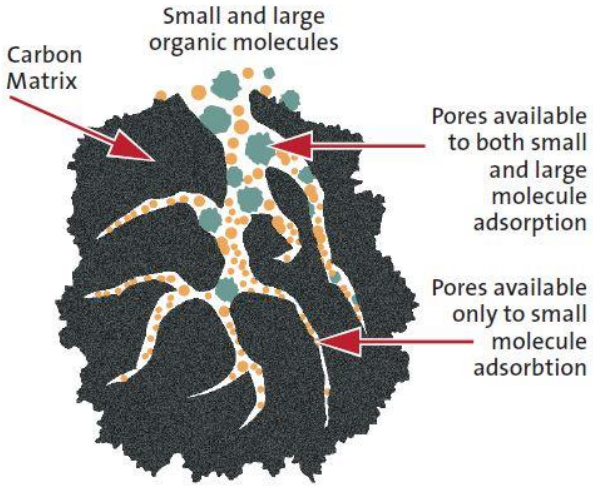

Figure 5: Activated carbon adsorption sites

For application in swimming pool water treatment another kind of filters very popular take advantages from the use of Diatomaceous earths (DE), a natural powder like material constituted of the shells of microscopic organisms called diatoms of variable diameters. Also called precoat filter, they must be equipped with rigid or elastic support, with external surface permeable, in which a layer of very fine grain size filter material is deposited.

The adsorption capacity of these filter exceeds the one of sand filters, blocking particles of dimension near 1 µm. But neither with this kind of filters is possible to block small molecules such as ammonia or Urea.

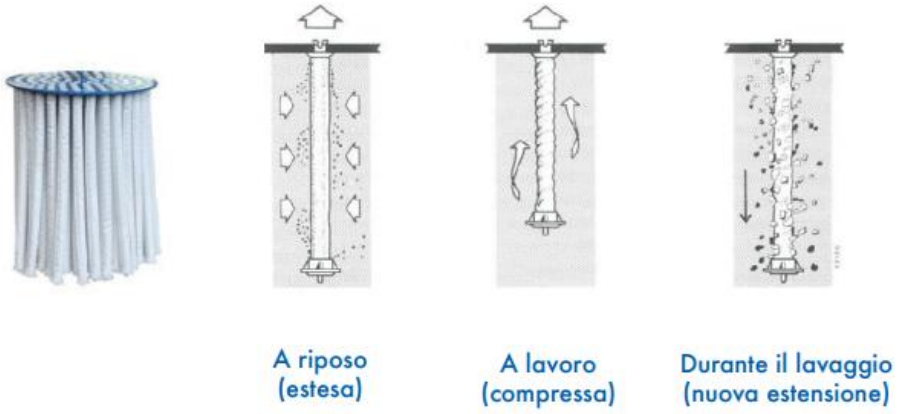

Figure 6: Diatomaceous earth filter working principle.

2 Carbon nanotubes

Carbon atoms have six electrons with two of them filling the 1*s* orbital while the remaining four electrons can fill the sp_3, sp_2 as well as the *sp* orbital depending on their hybridization, forming different bounded structures such as diamond, graphite, graphene, nanotubes, or fullerenes.

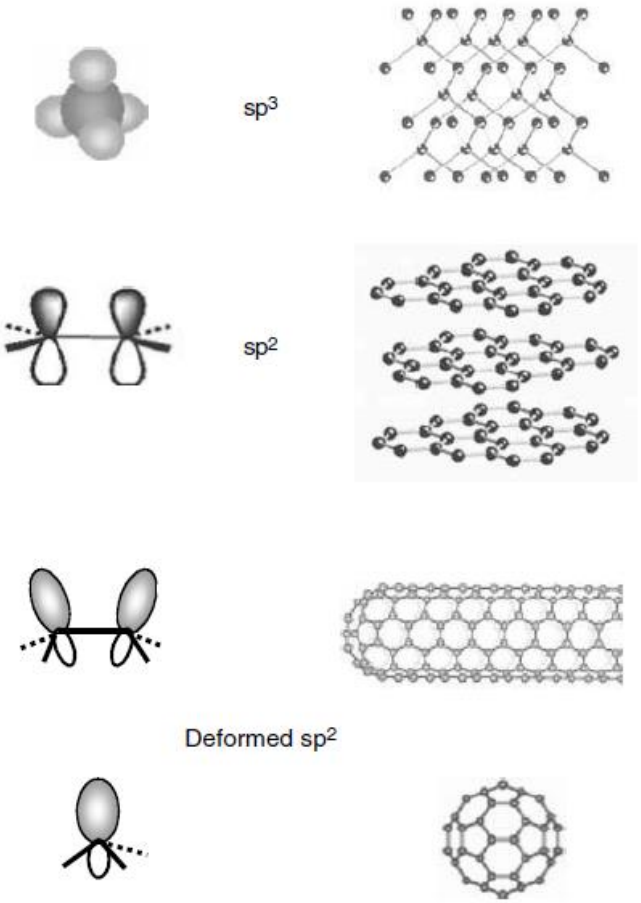

Figure 7: Bounded structures of carbon: diamond, graphite, nanotubes, and fullerenes.

In graphene, a planar hexagonal network is formed, three external electrons of each carbon atom occupy the planar sp_2 hybrid orbital and each bond is separated by an angle of 120° to form three in-plane σ bonds with an out-of-plane π orbital bond.

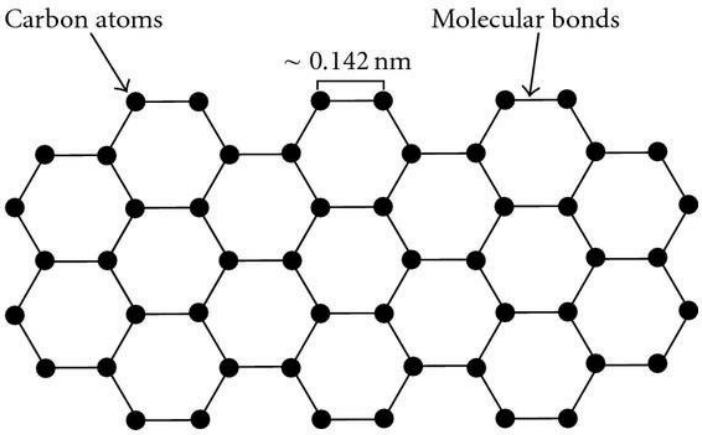

Figure 8: Graphene structure.

Graphene is considered a theoretically 2D structure and it is the base unit of nanostructured carbon allotropes.

In graphite, each plane of graphene is connected to another one with a spacing of 0.34 nm through van der Waals forces. It is very difficult to obtain just one isolated plane of graphene, sometimes is called graphene also structures with few layers.

Carbon Nanotubes (CNTs) are a particular theoretical 1D allotropic form of carbon, they can be imagined as hollow cylinders formed by rolling graphene sheets.

2.1 Discover

It is not easy to attribute to a single person the merit of the discover of carbon nanotubes, nowadays it is still subject of some controversy.

The first form of carbon nanotubes was reported by Sumio Lijima in is work, “Helical microtubes of graphitic carbon”, published by Nature in 1991.

In the intent of produce Carbon Fullerenes C60 with Arc-discharge evaporation technique he casually creates a new form of carbon consisting of needle-like tubes. [14]

Fullerenes C60 are made of 20 hexagons and 12 pentagons, given by a mixture of sp^2 with sp^3 bonds to gives a spheroidal structure.

Multi wall carbon nanotubes (MWCNTs) of Lijima were the first example of this kind of graphitic structure, the identification of a single wall carbon nanotubes (SWCNTs) requires a few years more.

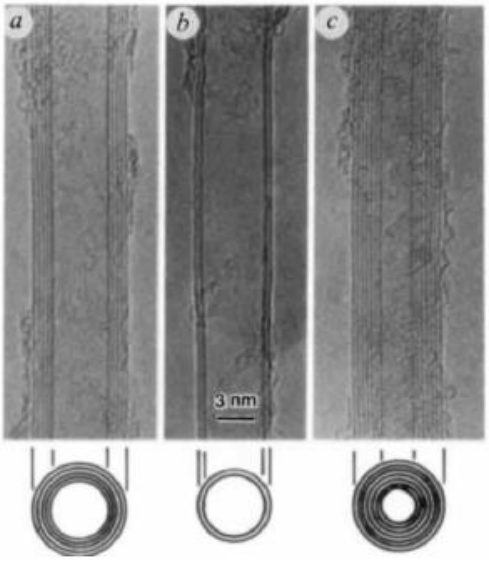

Figure 9: Electron micrograph of microtubules of graphitic carbon by Lijima. [14]

Although the first transmission electron microscope (TEM) evidence for the tubular nature of some nanosized carbon filaments is believed to have appeared in 1952 in the Journal of Physical Chemistry of Russia, SWCNTs was firstly described in two different papers published on NATURE in 1993, one by Lijima and Ichihashi, at the time affiliated at NEC, the other by Bethune et al. from IBM, California. [15]

The impact of this discovery was evidence from the beginning. from 1990 to 2003 considerable efforts have been made in the development of new synthesis methods of nanotube production and related test equipment for fabrication of high quality nanotubes and nanofibers. The total number of publications in this period (14 years) was 351,824 papers. Carbon nanotubes rapidly supplanted fullerenes as one of the hottest research topic of the Twentieth Century. [16]

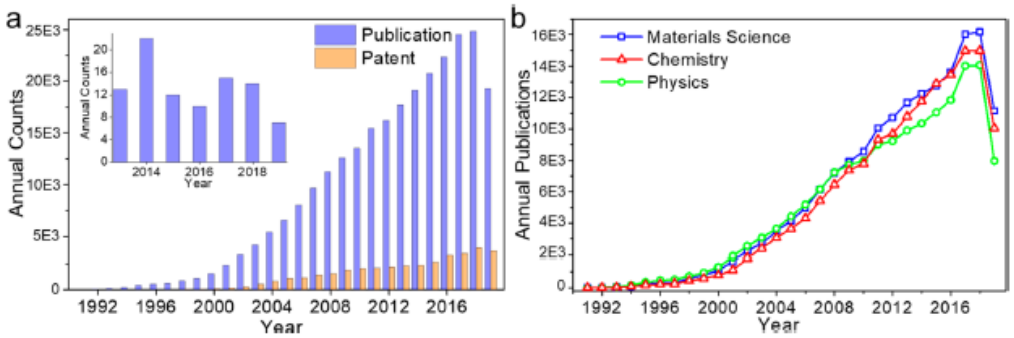

Figure 10: Trends in research on CNTs (Data from ISI Web of Science on December 7, 2019).

2.2 Structure

SWCNTs can be ideally constructed starting from a graphene sheet, in which carbon atoms are organized in a honeycomb lattice.

Two vectors, $\mathbf{a_1}$ and $\mathbf{a_2}$ form the graphene base for carbon nanotubes as shown in figure 11, they are not orthogonal but an angle of 60° is formed between them.

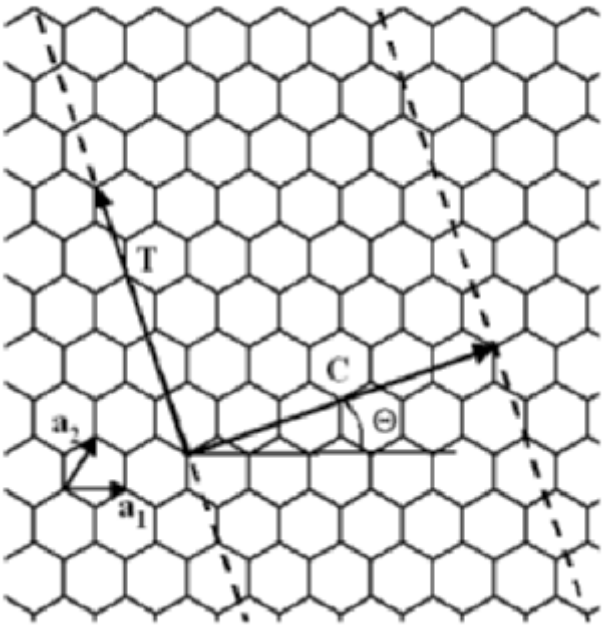

Figure 11: The principle of nanotube construction from a graphene sheet.

This construction allows to characterize completely the CNT structure with a pair of two integers (n, m).

The so-called chiral vector **C** is defined as follow:

$$\mathbf{C} = \mathrm{n}\mathbf{a_1} + \mathrm{m}\mathbf{a_2}$$

It joins two crystallographically equivalent sites of the nanotube on the graphene sheet.

The modulus of **C** could be evaluated by means of Carnot Theorem:

$$|\mathbf{C}| = \mathrm{a}_0\sqrt{\mathrm{n}^2 + \mathrm{m}^2 + \mathrm{nm}}$$

Where a_0 ≈ 1.42 Å is the lattice parameter of graphene.

Noting that the modulus of the chiral vector is equal to the circumference of the nanotube, the diameter of the tube can be defined as:

$$\mathrm{d_t} = \frac{\mathbf{C}}{\pi}$$

A vector **T** perpendicular to the chiral vector, can define the period along the direction parallel to the growth axis.

The tube unit cell is so defined by a cylinder of circumference **C** and height **T**.

The hexagons orientation on the tube surface is characterized by the angle θ, named the chiral angle, defined as:

$$\theta = \arctan\left(\frac{\sqrt{3}\mathrm{m}}{2\mathrm{n} + \mathrm{m}}\right)$$

It is practically the angle formed between $\mathbf{a_1}$ and **C.**

Furthermore, it is possible to classify Ideal SWCNTs depending on how the graphene sheet is rolled up, three possible crystallographic configurations can be identified:

- zig-zag
- armchair
- chiral

In these configuration θ assumes different values, it values 0° for zig-zag tubes (m = 0) in which two opposite C–C bonds of each hexagon are parallel to the tube axis, 30° for armchair ones (m = n) in which the C–C bonds are perpendicular to the axis, while all the angles between 0° and 30° define chiral nanotubes. It is

possible to consider just the first 30° due to the periodicity of the lattice (n ≥ m is used for convention). [17] [18].

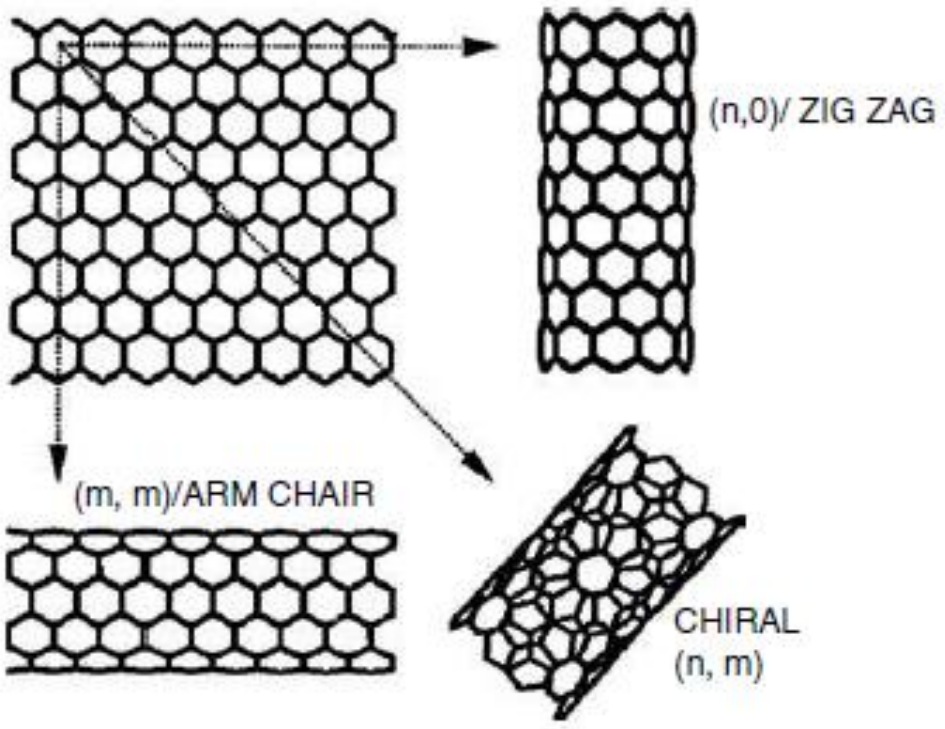

Figure 12: zig zag, armchair, chiral nanotubes.

Single wall carbon nanotubes usually assemble in bundles to minimize their energy through *van der Waals interactions,* it is very difficult to find them as isolated objects.

Nanotubes can also be obtained as multi wall carbon nanotubes, which are concentric SWNTs, the interlayer tubule is about 3,4 Å, that is the inter-sheet distance in hexagonal graphite. [17]

Furthermore, in real CNTs are present numerous local defects, for example topological defects such as pentagons (inducing positive curvature) and heptagons (inducing negative curvature) can be incorporated into the hexagonal network to form capped, bent, toroidal and helical nanotubes [19]

2.3 Properties

Carbon nanotubes exhibit outstanding features for what concern mechanical, electronic, optical, thermal properties and many others with still a lot of research active on investigate them.

Due to its hollow structure, CNTs has also large specific surface area, high pore volume, high aspect ratio, hydrophobic walls and stable chemical properties, qualities that make them interesting as absorbent material.

Anyway, carbon nanotubes cannot be dispersed in the environment, several studies indicate that they are toxic to organisms and human beings. [20]

Mechanical properties

The carbon nanotubes are expected to have high stiffness and axial strength as a result of the carbon-carbon sp2 bonding, in fact σ bonding is the strongest in nature. [21]

Both experimental measurements and theoretical calculations agree that nanotubes are stiffer than diamond.

Young's modulus is independent of tube chirality, but dependent on tube diameter, the highest value is from tube diameter between 1 and 2 nm. [19]

The elastic response of a nanotube to deformation is also very remarkable, most hard materials fail with a strain of 1% or less due to propagation of dislocations and defects, both theory and experiment show that CNTs can sustain up to 15% tensile strain before fracture. [19]

	Young's modulus (GPa)	Tensile Strength (GPa)	Density (g/cm^3)
MWNT	1200	~150	2.6
SWNT	1054	75	1.3
SWNT bundle	563	~150	1.3
Graphite (in-plane)	350	2.5	2.6
Steel	208	0.4	7.8

Figure 13: Mechanical properties of CNTs. [19]

Electronic properties

The electronic properties of carbon nanotubes directly derive from their band structure, it is possible to determine the band structure of a SWCNTs and identify if a nanotube behaves as a moderate bandgap semiconductor or a metallic material using the π-tight-binding model within the zone-folding scheme depending on the indices n and m.

For MWCNTs result more difficult modelling the band gap as more variable must be considered.

As a starting point the band structure of a single graphene sheet is considered, curvature effects are neglected, the Huckel model can be adequate to represents that situation with boundary conditions making CNTs periodic under translation along the chiral vector.

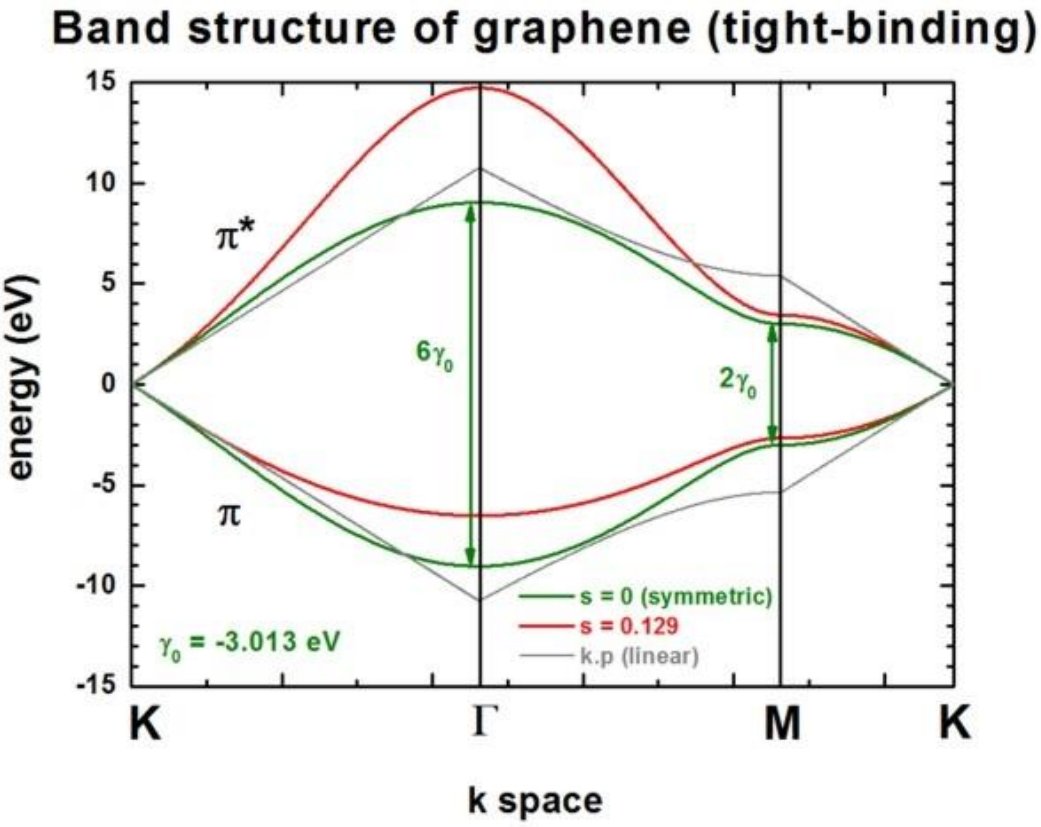

Figure 14: Band structure of graphene.

From the figure it is possible to see that there is a point in the graphene band structure that has zero-energy gap, it is named K-point, in this point the behaviour is the same of a metallic material.

Easily, it is possible to solve the Huckel problem to give the one-electron eigenvalues as a function of the two-dimensional wavevector **k** in the hexagonal Brillouin zone of graphene in terms of the primitive lattice vector $\mathbf{a_1}$ and $\mathbf{a_2}$, with just one hopping parameter γ_0.

$$\epsilon(\mathbf{k}) = \gamma_0 \sqrt{3 + 2\cos(\mathbf{k}\cdot\mathbf{a_1}) + 2\cos(\mathbf{k}\cdot\mathbf{a_2}) + 2\cos\big(\mathbf{k}\cdot(\mathbf{a_1}-\mathbf{a_2})\big)}$$

The allowed electronic states are then restricted to that included in the graphene first Brillouin zone by the born-von Karman boundary condition.

$$\boldsymbol{k}\cdot\boldsymbol{C} = 2\pi\mathrm{m}$$

In which m is an integer.

The allowed states lie along parallel lines, representing the quantization along the axial direction that is a quasi-continuum, separated by a distance of $\frac{2\pi}{\boldsymbol{C}}$. [22]

To study the condition of metallicity of a carbon nanotube is necessary to superimpose the plot of the allowed wavevector with the structure of graphene in the reciprocal space, to have a metallic nanotube, one allowed wavevector must touch the K-point.

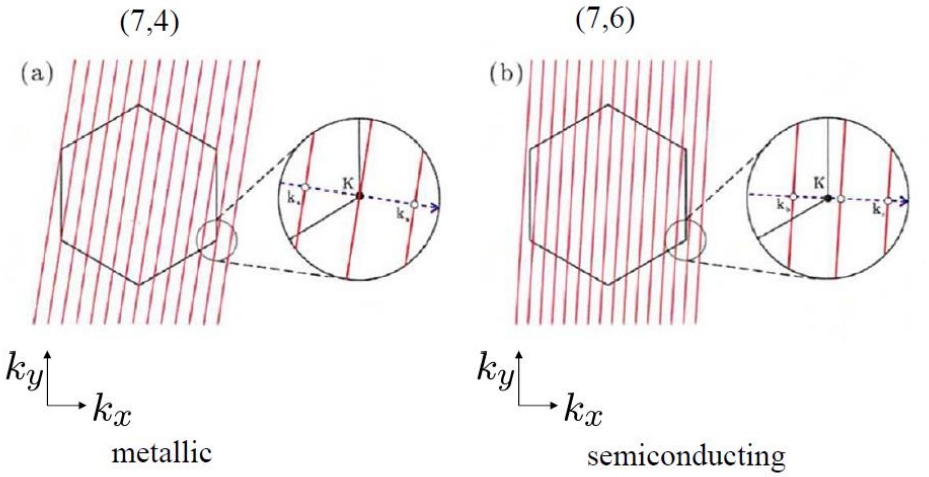

Figure 15: Metallic condition for carbon nanotubes.

All armchair SWCNTs and one-third of all zigzag nanotubes are metallic, the rest are semiconducting.

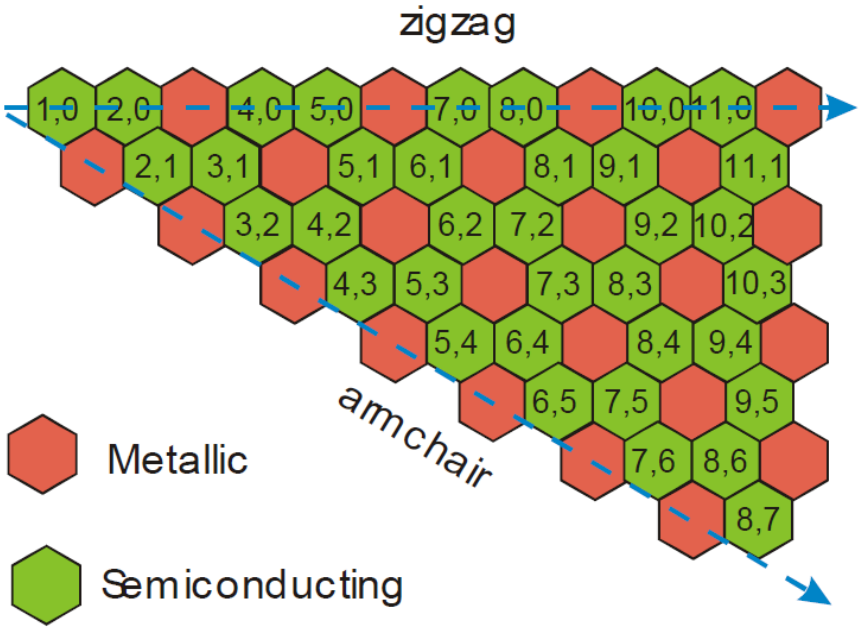

Figure 16: Metallic and semiconducting nanotubes.

Optical properties

Defect-free nanotubes, especially SWCNTs, offer direct band gap and well-defined band and subbands structure, which is ideal for optical and optoelectronic applications.

Usually, as-grown nanotube samples are a mixture of semiconducting and metallic tubes, optical spectra have been extensively used to determine the detailed composition of SWCNT samples.

Optical and optoelectronic properties can be understood from the band structure or DOS of a SWCNT.

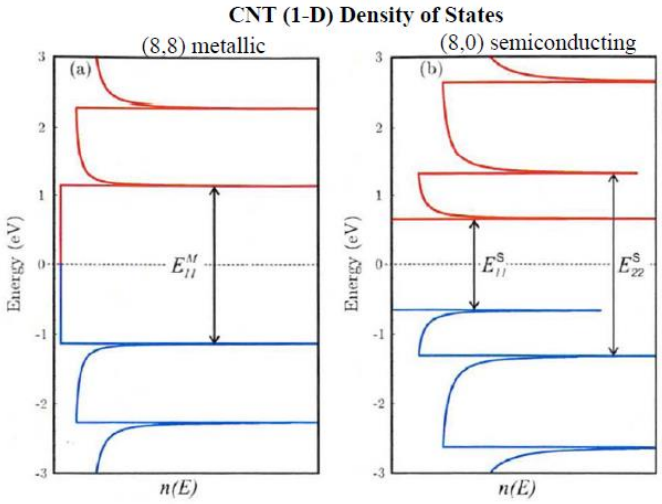

Figure 17: Density of states of metallic (8,8) and semiconducting (8,0) carbon nanotubes.

For metallic nanotubes is possible to see the absence of a gap in energy, the peaks of DOS are called van Hove singularity (VHS).

The optical transition occurs when electrons or holes are excited from one energy level to another, the wavelength of a semiconducting tube can vary from 300 to 3000 nm, this suggests potential applications of semiconducting nanotubes in optical devices from blue lasers to IR detectors.

Raman spectrum of CNTs shows two sharp peaks, the peak near 1334 cm^{-1} is the so-called D-band which is related to disordered sp_2-hybridized carbon atoms of CNTs, while the peak near 1582 cm^{-1} is the so-called G-band which is related to the structure integrity of sp_2-hybridized carbon atoms of the CNTs. [23]

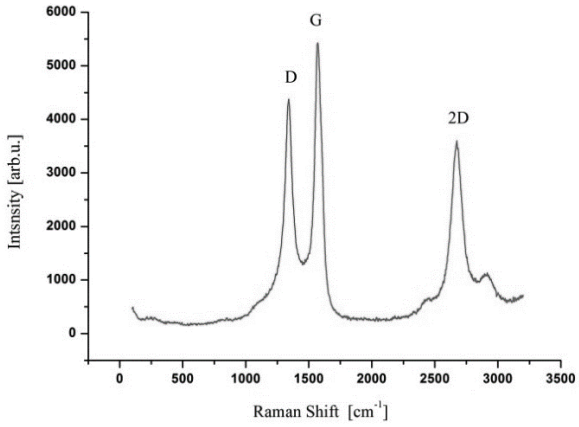

Figure 18: Example of Raman spectra of MWCNTs

2.4 Synthesis Processes

Carbon nanostructures can be synthesized principally via three main processes: arc-discharge, laser ablation and chemical vapor deposition (CVD).

Apparatus for the three different processes is schematically displayed in the figure below. [24]

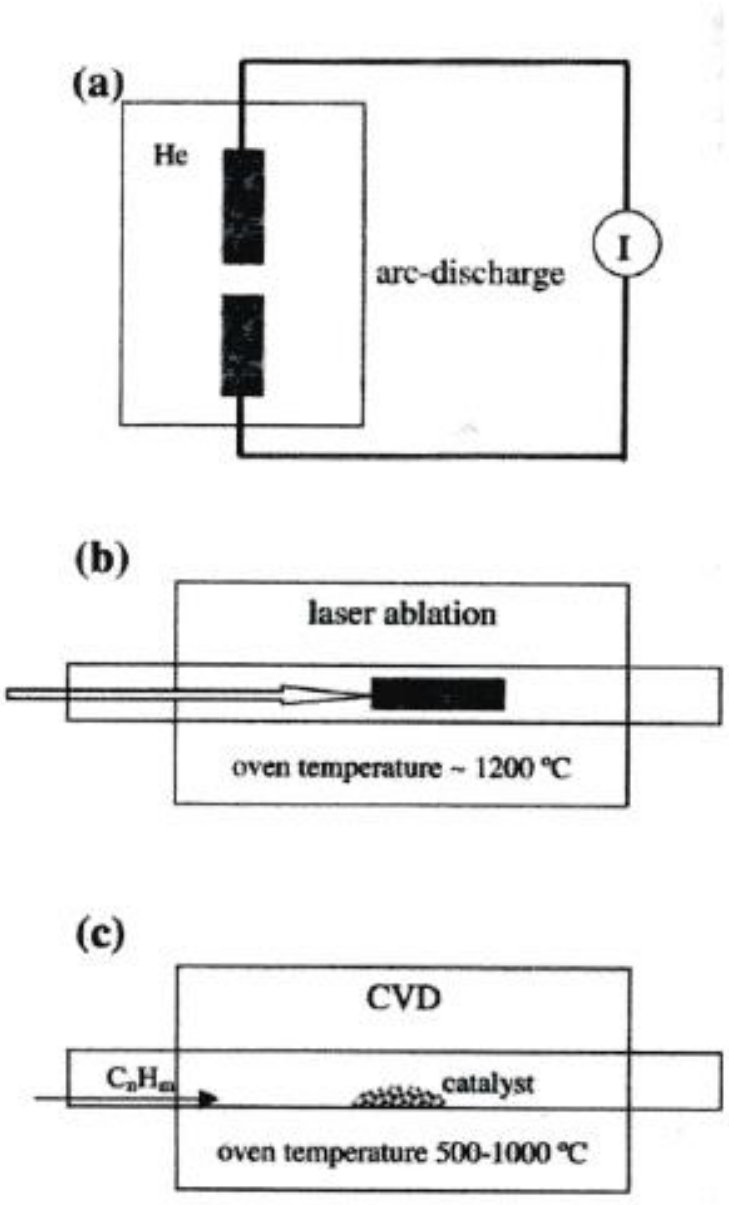

Figure 19: Schematic representation of the CNT synthesis apparatus.

For the synthesis of carbon nanotubes, the mostly used methods required vacuum systems and sophisticated inert gas handling system, pump system, etc. with an increasing of the cost of production. Find soft condition of synthesis is one of the major goal of research groups.

All common methods of synthesis require similar catalysts to grow CNTs, therefore, they might share a common growth mechanism, that nowadays is still not completely clear.

The overall process involves three main steps:

1. carbon feedstock is supplied on catalyst surface to get fullerenes as intermediate
2. small carbon fragments like C_2 and C_3 are generated from the decomposition of hydrocarbons by heat and subsequently are deposited on catalyst surface
3. nanotube grows until the catalyst surface is fully covered with excess carbon, its catalytic activity ceases and the CNT growth is stopped.

The synthetized tubes are then separated from each other as SWCNTs or MWCNTs, and the individual nanotube is purified and transferred to a predefined area of target substrate.

Currently the common method widely accepted in the synthesis of CNTs for large-scale and almost pure industrial production is the CVD method due to its simplicity and low cost compared to the others.

The laser ablation method is more expensive than either arc discharge or chemical vapor deposition. Anyway, SWCNTs produced by the Pulsed Laser Vaporization method are of excellent structural integrity, long, and of high purity. [25]

2.4.1 CVD

CVD is the most versatile and promising technique both for bulk production and for direct device integration.

During the chemical synthesis of CNTs the formation of different carbonaceous materials can occur including the desired MWCNTs and SWCNTs in one hand, and amorphous carbon and metal particles encapsulated by graphitic shells on the other hand which are not desire structures. [26]

The mainly used carbon sources for CVD synthesis of CNTs are fossil-based hydrocarbons and plant-based hydrocarbons, anyway there are continuous attempts to try to find more ecological sources.

Among fossil fuel hydrocarbon methane, ethylene, natural gas, acetylene, benzene etc. are conventional carbon sources which are widely used for CNTs research and industrial production.

On the other hand, transition metal nanoparticles are principally used as catalysts for the growth of CNTs, however, recently CNTs are also grown from ceramic nanoparticle catalysts, noble metals, and semiconducting nanoparticles.

Arash Yahyazadeh et al. synthetized multi walled carbon nanotubes of 1.2 μm in length using methane as economical and non-toxic carbon source and ferrocene and molybdenum hexacarbonyl as thin layer catalyst nanoparticle precursors, with significant carbon yield of 75.4% which represents high catalyst activity at 750 °C for 35 min. [26]

For the growth of CNTs by CVD the formation of nanoparticles of metal catalysts are necessary on the surfaces of non-conducting substrates including alumina, silicon and magnesium oxide.

The nucleation of catalyst is usually carried out via chemical etching (using ammonia) or thermal annealing.

The pre-treated supported material is then placed in a tabular reactor for the growth process, The reactor is usually made in quartz to support the high temperature of reaction.

After the reactor/furnace is heated to the sufficient reaction temperature (600–1200 °C), a mixture of hydrocarbon gas (ethylene, methane, acetylene etc.) and a process gas (nitrogen, hydrogen, argon) is injected to react in a reaction chamber over the surface of metal catalysts for a given time period (usually 15–60 min) making the decomposition of the carbon precursor taking place.

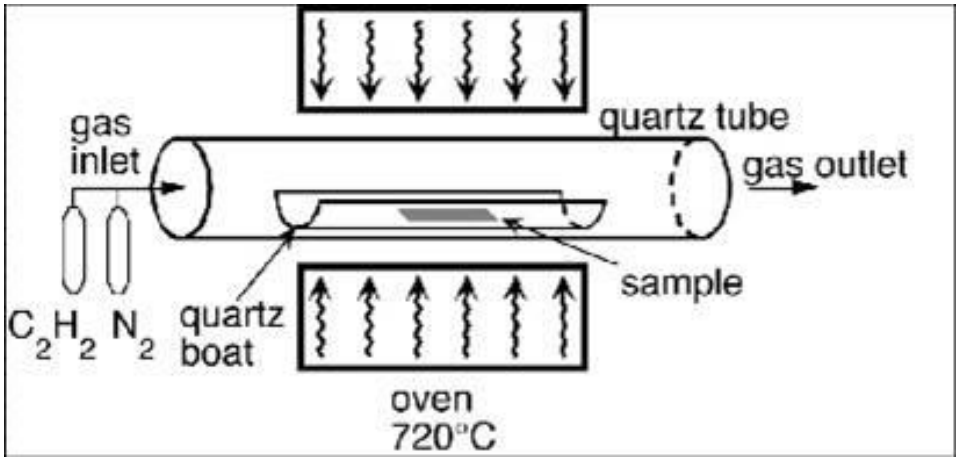

Figure 20: CVD apparatus.

There are nowadays two accepted mechanisms for growth of CNTs, VLS (vapour-liquid-solid) and VSS (vapour-solid-solid).

In VLS mechanism firstly a hydrocarbon gas adsorbs and dissociates on the surface of the catalyst particle to form elementary carbon atoms, secondly the carbon atoms dissolve in the bulk of the nanoparticle catalyst to form liquid metastable carbide and then diffuses within the particle. Lastly the solid carbon precipitates at the rare end of the particle to form a carbon nanotube.

In VSS mechanism the gas hydrocarbon first dissociates and then the dissociated carbon atoms diffuse on the catalyst particle and lastly the carbon precipitates in the form of nanotube.

Furthermore, the growth mechanisms of CNTs in the CVD process have been generally divided into two distinct methods: base/root growth and tip growth.

In root growth, the catalyst particle stays pinned at the support surface due to the strong interaction between the substrate and the catalyst, the nanotubes grow above.

On the contrary, the tip-growth mechanism takes place when the catalyst is lifted off from the support surface during CNT growth due to weak support–catalyst interaction.

The main parameters affecting CNT growth in CVD are the atmosphere, the carbon source, the arrangement of catalytic sites and its preparation, the nature of substrates and the growth temperature.

Growth temperature

Low-temperature (300–800 °C) yields MWCNTs, whereas a higher temperature (600–1150 °C) of reaction favours SWCNTs growth, because the SWCNTs have higher energy of formation than MWCNTs.

Carbon sources

The molecular structure of the carbon source strongly effects the morphology of the CNTs produced.

Linear hydrocarbons like methane, ethylene, acetylene etc. produce straight hollow CNTs as they thermally decompose into atomic carbons or linear dimers/ trimers of carbon, whereas cyclic hydrocarbons like benzene, xylene, fullerene, cyclohexene etc. produce relatively curved CNTs.

Catalysts

In CVD synthesis of CNTs, catalysts play a very important role and by improving the desired characteristics of a catalyst the yield as well as the quality of CNTs can be improved.

Usually transition metal nanoparticles are employed as catalysts, they act as nucleation sites for CNT growth.

Generally, nanometre-size particles as catalysts are required to synthesize SWCNTs whereas, MWCNTS can also be produced without catalysts. The catalyst-particle size dictates the tube diameter, when the size of the catalyst particle is a few nm SWCNTs are formed, whereas particles a few tens nm wide favours MWCNT formation.

The function of the catalyst is to decompose hydrocarbons at lower temperature than the spontaneous decomposition temperature of hydrocarbon via heat and its new nucleation to form CNTs. It is the CNT–CNT or CNT–substrate interactions in addition to the arrangement and activity of catalytic sites that determine if CNTs grow in an isolated, tangled, or aligned configuration.

Transition metals (usually Fe, Co, Ni) in the form of nanoparticles are found to be most effective catalysts due to two principal reasons:

- At high temperature, carbon has high solubility in these metals.
- Carbon has high diffusion rate in these metals.

Substrates

The material of the substrate, its surface morphology and texture properties affect the yield and quality of the grown CNTs.

Chemical interactions between the catalyst particles and surface groups of the substrate can also aid in maintaining the size distribution of the catalyst particles during growth of CNTs.

Various substrates used in CVD for the growth of CNT are silicon, silicon carbide, graphite, quartz, silica, alumina, magnesium oxide, calcium carbonate ($CaCO_3$), zeolite and NaCl etc.

The grain boundary or crystalline steps of the support material play a very important role in CNT growth and orientation. The direction of the CNT growth is governed by the crystallographic orientation of the exposed substrate surface.

A general pre-condition for a support material is the thermal and chemical stability under growth process. [18]

In literature there are plenty of example of carbon nanotubes synthesis by CVD methods, here will be reported the work by Policicchio et al. which have produced MWCNTs with Co-Fe catalyst in a quartz tube reactor with a reaction temperature of 700° C and ethylene (C_2H_4) as carbon source, in a way similar to that used by Innovacarbon SRL to produce its own carbon nanotubes. [27]

The advantages of CVD include:

- It is a simple, economical and scalable technique for mass production of carbon nanotubes.
- It utilizes plenty of hydrocarbons in any form that is solid, liquid or gas and various substrates.
- It can be used to grow CNTs in different forms like aligned or entangled, straight or coiled nanotubes or a desired architecture of nanotubes on pre-defined cites of a patterned substrate.

2.4.2 Laser ablation

The laser ablation method can be applied to graphite or other carbon sources in order to obtain a wide variety of carbon allotropes, such as diamond-like carbon films, fullerene carbon molecules, carbon nanotubes and graphene.

Carbon atoms have the unique ability to congregate into miscellaneous nanostructures under the conditions of laser vaporization.

Pulsed lasers are especially suitable in generation of non-equilibrium conditions due to a short time scale of temperature changes.

During the interaction of the laser beam with a target, its surface is heated to a temperature exceeding the boiling point and sometimes exceeding the critical temperature, at the same time, the vaporization begins. The evaporated particles are further heated by the laser pulse to temperatures of several tens of kilokelvin and form a plasma plume.

Next, the expansion of the plasma plume takes place. When the plasma cools during expansion along a step temperature gradient, carbon and catalyst metal atoms condense into larger structures.

In the laser vaporization method, both continuous wave lasers and pulsed lasers are successfully used, usually, 1064 or 532 nm Nd:YAG lasers are applied although 248 nm KrF lasers were also used with success. [25]

The growth conditions change considerably with the laser fluence, Chrzanowska et al. studies the effect of laser wavelength on the single-wall carbon nanotubes synthesis, A double pulse Nd:YAG laser, working at a wavelength of 355 or 1064 nm, was used in this experiment, they observe that the useful range of the UV laser radiation fluence is narrower and the properties of synthesized nanotubes depend much more on the laser fluence than in the case of infrared laser radiation. [25]

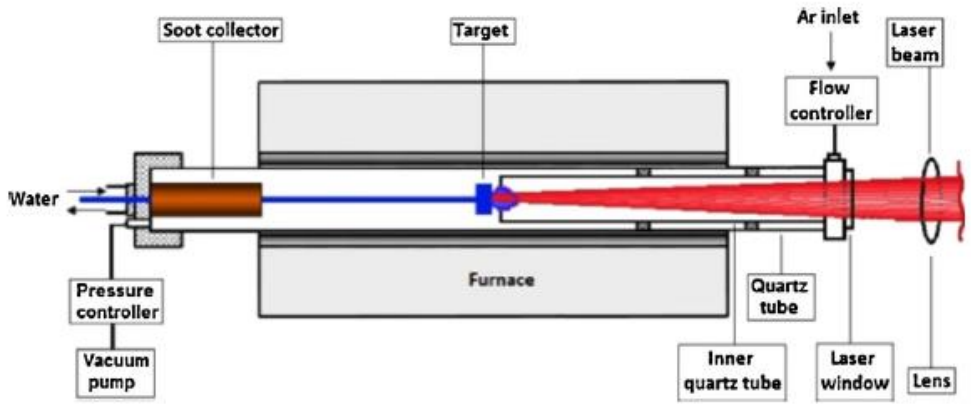

Figure 21: Reactor for carbon nanotube synthesis by the laser ablation method.

2.4.3 Arc-discharge

Arc-discharge method (AD) was firstly practiced for the synthesis of fullerenes, the major benefit of this technique is the production of a large quantity of CNT and fewer structural defects than those produced by lower temperature techniques.

The main drawback of AD is its poor control effect over the CNTs chirality, which is important for their characterization and application. [28]

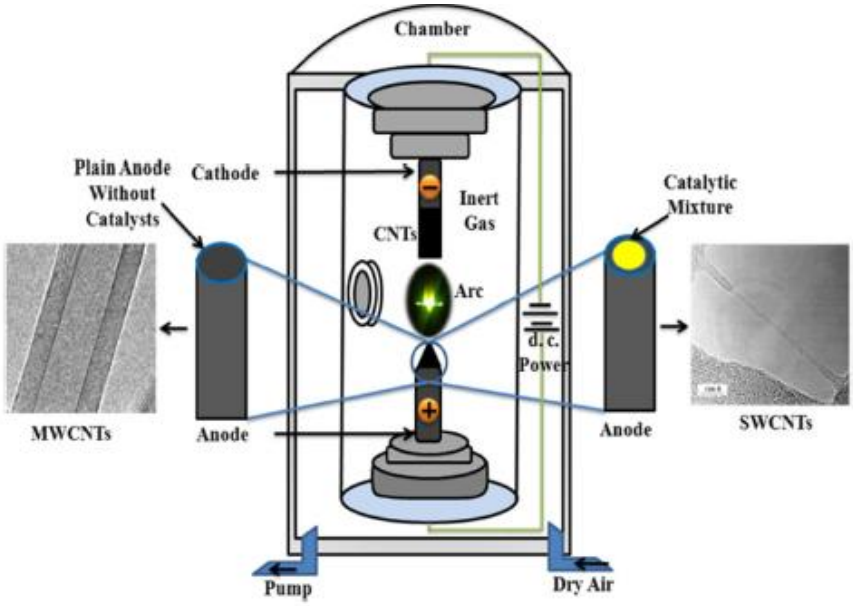

Figure 22: Arc discharge apparatus.

In the arc-discharge set-up, two graphite rods of 7 and 20 mm in diameters are used as anode and cathode electrodes, respectively. An arc is produced in between the electrodes by a DC power supply capable to provide 100–200 A current voltage range 20–30 V.

Arc is produced manually between electrodes for time less than 1 minute after that the two electrodes are brought to a certain distance to terminate the operation.

Under the effect of arc, anode electrode sublimates and carbon deposits on the cathode electrode in the form of carbon nanotubes and other form of carbon.

3 Adsorption

The change in concentration of a given substance at the interface with respect to that of neighbouring phases is referred to as adsorption.

The material that will be retained is defined as the adsorbate, while the penetration by the molecules into the bulk solid phase is called absorption.

Depending on the type of phases in contact, the following systems can be considered:

- liquid-gas
- liquid-liquid
- solid-solid
- solid-liquid
- solid-gas.

The present work will be focused upon a solid-liquid adsorption system.

Usually, the small particles of adsorbent are held in a fixed bed, and fluid is passed continuously through the bed until the solid is nearly saturated and the desired separation can no longer be achieved.

When discussing the fundamentals of adsorption, it is useful to make a distinction between physical adsorption (physisorption), which involves only relatively weak intermolecular forces, and chemical adsorption (chemisorption), which involves, the formation of a chemical bond between the sorbate molecule and the surface of the adsorbent.

Anyway, there are many intermediate cases and usually it is not possible to categorise a particular system unequivocally, most of the time different kinds of adsorption mechanism occur simultaneously.

Instances of physisorption, such as van der Waals' interactions, are usually at binding energy lower than 20 kJ/mol. Electrostatic interactions range from 20 to 80 kJ/mol and are also frequently classified as physisorption. Chemisorption bond strengths can range at around 80–450 kJ/mol. [29]

Chemical bonds are apparently stronger than physical adsorption, but the ratio of these interactions depends on the number of functional groups and the surface contributing to the adsorption.

To establish if an adsorption process is chemical or physical, it is necessary to prove the formation of some chemical bonds using some analytical techniques (FTIR, Raman spectroscopy, TGA, and so on) combined with thermodynamical data of changes in enthalpy (ΔH) and changes in entropy (ΔS).

It is expected that large organic molecules would be adsorbed by physical interactions and small inorganic ions could be complexed with nitrogen or oxygen atoms of amine, amide, phenols, alcohols, and so on, being an interaction with adsorbent, which is a chemical adsorption process. [30]

3.1 Adsorption mechanisms

The process of adsorption falls into four basic stages:

- Transport of the adsorbate from the bulk solution to the film of solvent around the particles of the adsorbent.
- Diffusive mass transfer of the adsorbate through the film.
- Intraparticle diffusion of the adsorbate through the pores of the adsorbent.
- Binding of the adsorbate to the active sites in the pores of the adsorbent.

The diffusive mechanism could be explained by the Weber-Morris intraparticle diffusion model:

$$q_t = k_{id}\sqrt{t} + \mathrm{C}$$

The adsorption process showed three zones which could be attributed to each linear portion.

The first linear portion (1st zone) was assigned to the diffusional process of the dye on the adsorbent surface. hence, it was the fastest sorption stage.

The second portion (2nd zone) was ascribed to intraparticle diffusion, a delayed process.

The third stage (3rd zone) could be regarded as the diffusion through smaller pores, which is followed by the establishment of equilibrium. [30]

Gamze Ersan et al. demonstrate the applicability of Weber-Morris model for adsorption of phenanthrene (PNT) by SWCNTs and MWCNTs. [31]

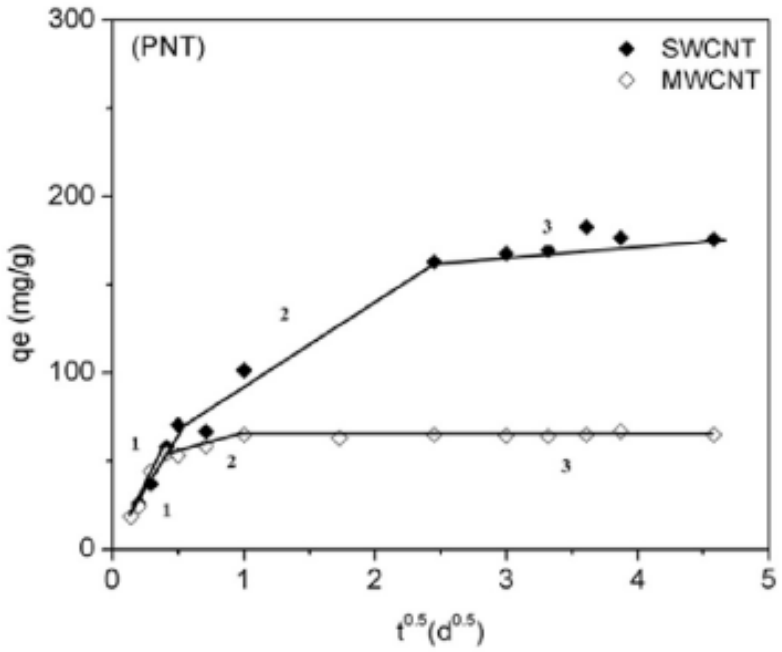

Figure 23: Weber-Morris model of adsorption of PNT by SWCNTs and MWCNTs.

The main factors that could have influence on the adsorption processes are:

- morphology and textural properties of adsorbents
- initial concentrations of adsorbate
- pH of the adsorbate
- contact time
- temperature
- adsorbent dosage
- agitation speed

Morphology and textural properties of adsorbents

The textural properties of the adsorbents such as pore size, total pore volume and superficial area are important factors that influence the adsorption process because adsorption is a surface phenomenon.

Most of the adsorbent materials are highly porous, due to the fact that usually the pores are very small, the internal surface area is orders of magnitude greater

than the external one. Higher surface area and higher pore volume of the adsorbent will yield to higher sorption capacity also for small species such as gases and inorganic ions.

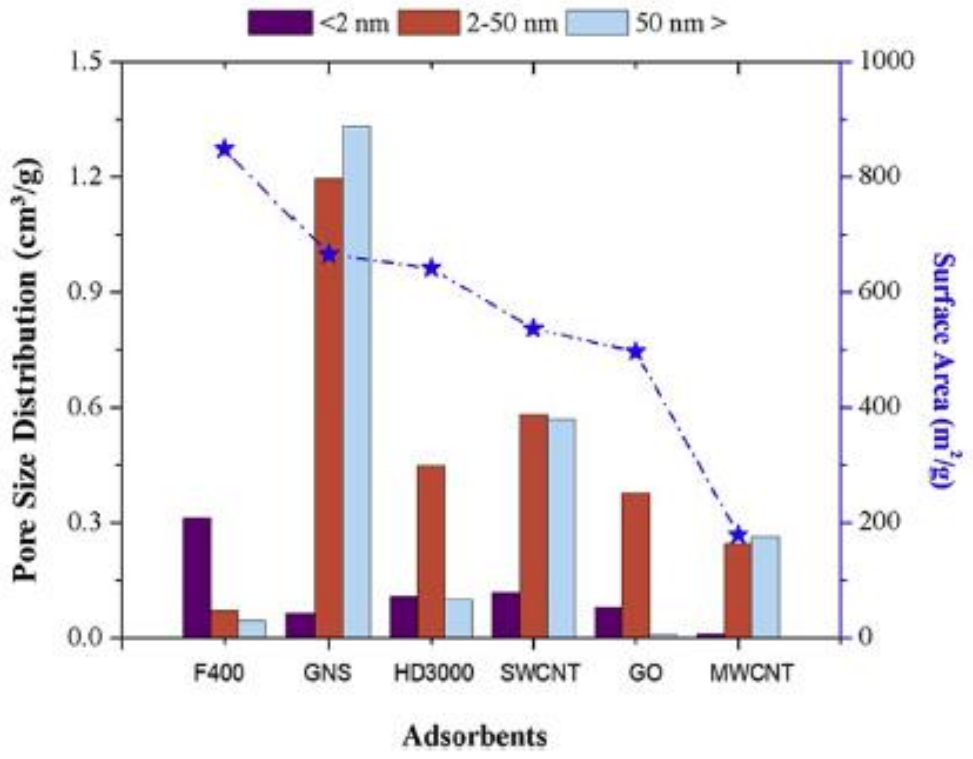

Figure 24: Pore size distribution and surface area for different carbonaceous materials. [31]

When nanomaterials are used as adsorbent, interactions between functional groups of the pollutant and the active sites of a nanomaterial are required, they are influenced by the textural and structural properties of the adsorbent.

The structural characteristic is also important, the arrangement of atoms and electronic properties of the adsorbent also present an important role in the adsorption process, mainly with the carbon nano adsorbents, such as graphene-family as well as nanotubes.

Initial concentrations of adsorbate

The initial concentration (C_o) of pollutant is an important parameter, fixing an amount of adsorbent, it is possible to obtain information about its maximum adsorption capacity.

Usually, increasing the initial adsorbate concentration would lead to an increase in the performance, until the adsorbent gets saturated.

For adsorbate solutions with lower concentration, the initial sorption rate is faster and an increase in the initial concentration leads to an increase in the time necessary to attain the equilibrium.

But another aspect should be considered, the mass diffusivity decreases with decreasing concentration under very dilute solution and causes the decrease in diffusion flux of adsorbate onto the surface of the adsorbent. [23]

It has been observed by O. Moradi in his study of ammonium ion adsorption by multi-walled carbon nanotube that varying the initial ammonium concentration in the range of 100–140 mg/L at 298 K with 0.05 g carbon nanotube at 35 min, ammonium ion adsorption capacity decreased with decreasing initial ammonium ion concentration in solution. [32]

pH of the adsorbate

One of the most influential factors in adsorption studies is the effect of pH of the adsorbate solution. Different adsorbates have different suitable pH ranges, depending on the adsorbent used.

It is possible to know if the surface of an adsorbent is positively or negatively charged depending on pH. The point of zero charge (pH_{PZC}) is the pH value required for surface of adsorbent to have a net neutral charge.

For pH values lower than pH_{PZC} the adsorbent presents a positive surface charge, as the distance in value between the pH and the pHPZC increases, the more positive the surface of the adsorbent will be. The adsorption of cations from adsorbate solution with pH values lower than the pH_{ZPC} is not favoured because of the occurrence of the electrostatic repulsion between the positively charged adsorbent surface and the cations, as well as the competition between H^+ and cations.

On the other hand, the adsorbent surface will be negative charged when pH of the adsorbate solution is greater than the pH_{ZPC} (alkaline pH), therefore, the functional groups on the adsorbent surface are deprotonated to form the negative charged surface, thereby favours adsorption of cations on the surface of the carbon adsorbent.

The pH_{PZC} of carbonaceous materials depends on acidic functional groups on their surface. The higher the concentration of acidic functional groups on the surface, the lower the pH_{PZC} value of carbonaceous materials. [30]

Contact time

During the kinetic adsorption studies, it is possible to measure the minimum time to attain the equilibrium. After this time, it is assumed that the system will remain at equilibrium.

It is useful to increase the contact time for the proper interaction between the adsorbent and adsorbate to guarantee equilibrium at higher concentration levels.

In an experiment conducted by Chungsying Lu et al. testing the adsorption properties of CNTs for THMs has been showed that a longer contact time is required to reach the equilibrium for more diluted solutions, this may be explained by the fact that diffusion mechanisms control the adsorption of THMs onto CNTs.

It is also noted that the smallest molecule, $CHCl_3$, is the most preferentially adsorbed onto CNTs, followed by $CHBrCl_2$, $CHBr_2Cl$ and then $CHBr_3$. This may be attributed to the fact that adsorption occurs with molecules that are small enough in size to enter the inner cavities through the pores. Therefore, the adsorption rate increases with decreasing size of the adsorbed molecules. [23]

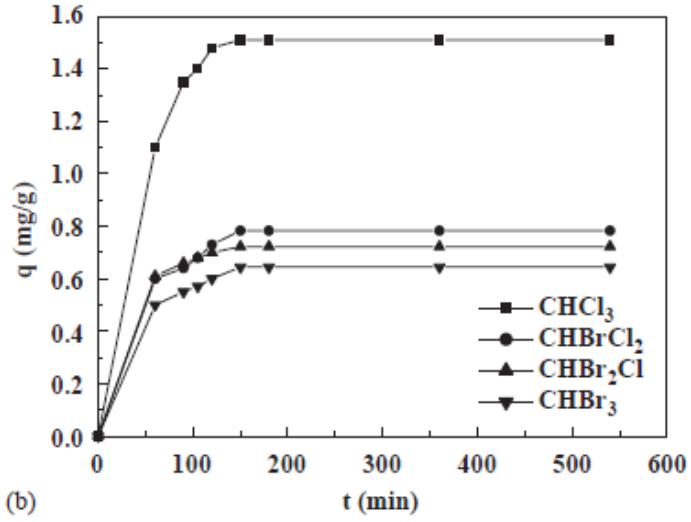

Figure 25: Effect of contact time on the adsorption of THMs with CNTs: C_0 = 3.2 mg/L [23].

Temperature

The temperature at which the adsorption process is carried out will influence both the rate of sorption and the degree in which sorption occurs.

An increase in temperature may lead to an increase in the kinetic energy and mobility of the molecules of the adsorbate and also increase the rate of intra-particle diffusion of the adsorbate.

In the adsorption process the effect of temperature on the system is reflected in the rate constant of adsorption. If adsorption studies are performed at different temperature values, one can obtain the value of the respective rate constants that can be used to evaluate the activation energy (E_a) of process using Arrhenius equation:

$$ln\, k = ln\, A - \frac{E_a}{RT}$$

Where k is the rate constant of the adsorption process; A is the Arrhenius constant; and E_a is the Arrhenius activation energy (kJ mol^{-1}) of the adsorption process, T is the absolute temperature (Kelvin), and R is the universal gas constant (8.314 J mol^{-1} K^{-1}).

E_a is important because it describes the nature of the interactions between the adsorbate molecule and the adsorbent.

Another important change that occurs when the temperature is increased is the equilibrium constants obtained from different isotherm models. An increase in temperature could decrease or increase the equilibrium constant of a pair of adsorbate/adsorbent. This observation affects the thermodynamics parameters of adsorption such as Gibb's free energy, enthalpy change and entropy change.

if an increase in temperature induces systematic increase in the equilibrium constant of an isotherm, the process of adsorption is endothermic. On the other hand, if an increase in temperature of the adsorption experiments bring about a decrease in the equilibrium constant, the process is exothermic.

O. Moradi et al. studies the influence of temperature in the adsorption capacity of MWCNTs powder to adsorb ammonium ions at 288–328 K with 10 mL, 140 mg/L NH^{+}_{4} solution and 0.05 g carbon nanotube. They found that the adsorption capacity decrease with increase in temperature, suggesting the process to be exothermic. [32]

Adsorbent dosage

Initially, an increase in adsorbent dosage tends to cause an increase in the percentage of removal, until a plateau is reached, and the curve is levelled off.

Increasing in the percentage of the adsorbate removal as the adsorbent dosages increase up to threshold value of adsorbent dosage could be attributed to increases in the adsorbent surface areas, augmenting the number of adsorption sites available for adsorption.

An increase in the adsorbent dosage leads to a decrease in q values.

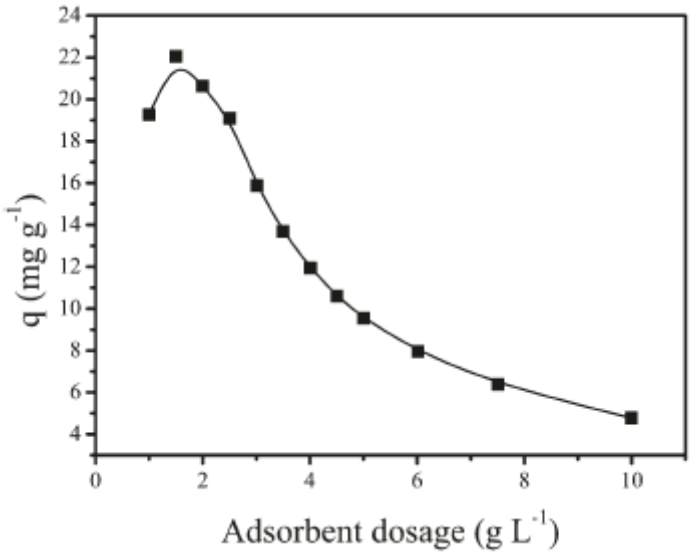

Figure 26: Effect of adsorbent dosage on the sorption capacity of an adsorbate using an adsorbent.

The adsorbent dosage must be fixed at the threshold value, which is the adsorbent dosage that corresponds to the minimum amount of adsorbent that leads to constant adsorbate removal.

Agitation speed

An adsorbent must interact properly with a given adsorbate before it can be adsorbed from solutions. Therefore, an adsorptive system must be reasonably agitated to bring adsorbate molecules closer to the active sites of adsorbents.

At extremely low or high agitation speed, adsorption process cannot be optimally achieved.

Elevated agitation speed could trigger desorption due to breaking down of adsorbate molecules.

Different pairs of adsorbate-adsorbent could have different optimum agitation speed, which could influence the adsorption capacity.

3.2 Equilibrium Isotherm Models

Adsorption isotherms are equations which describe the equilibrium relation between the quantity of the adsorbed material and the pressure or concentration in the bulk fluid phase at constant temperature. [33]

There are numerous equations for describing the adsorption equilibrium of an adsorbate on an adsorbent.

The amount of pollutant adsorbed can be calculated using the following equation:

$$q_e = \frac{(C_0 - C_e)V}{m}$$

where C_0 and C_e (mg/L) are the initial pollutant concentration and its concentration at equilibrium, respectively.

V is the volume of the solution (L) and m is the mass of adsorbent used (g).

At a constant temperature, an adsorption isotherm describes the relationship between the amount of adsorbate adsorbed by the adsorbent (q_e) and the adsorbate concentration remaining in solution after equilibrium is reached (C_e).

The most employed and discussed equilibrium isotherm in literature is the Langmuir equation, but other isotherm models such as Freundlich isotherm, Sips isotherm, Liu isotherm, Redlich–Peterson isotherm have also been studied for understanding the behaviour of CNTs as adsorbent material.

Langmuir Isotherm Model

The Langmuir isotherm describes a progressively increasing surface occupancy as a function of pressure, until the entire surface area is coated with a single layer of molecules and no further adsorption can occur. [34]

Assumptions:

- Adsorbates are chemically adsorbed at a fixed number of well-defined sites
- A monolayer of the adsorbate is formed over the surface of the adsorbent when it gets saturated
- Each site can hold only one adsorbate species
- All sites are energetically equivalent
- Interactions between the adsorbate species do not exist.

At equilibrium, the number of molecules being adsorbed will be equal to the number of molecules leaving the adsorbed state.

Langmuir isotherm equation:

$$q_e = \frac{Q_{max} K_L C_e}{1 + K_L C_e}$$

where q_e is the amount of pollutant adsorbed at the equilibrium (mg/g), C_e is the residual adsorbate concentration at the equilibrium(mg/L), K_L is the Langmuir equilibrium constant (L/mg), and Q_{max} is the maximum adsorption capacity of the adsorbent (mg/g). [30]

John-David R. Rocha et al. find a good fit of their data of adsorption of organic aromatic molecular by electronically sorted SWCNTs by means of chromatography technique using Langmuir model, suggesting that monolayer adsorption is taking place on a surface with a finite number of identical sites and uniform adsorption energies. They also found that semiconducting SWCNTs are more efficient than metallic SWCNTs. [35]

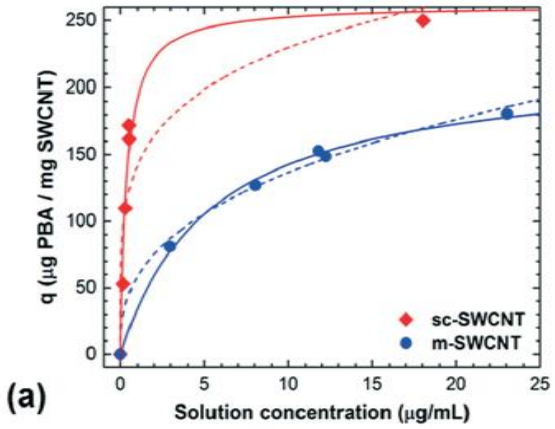

Figure 27: Equilibrium isotherms for adsorption o 1-pyrenebutyric acid using Langmuir (solid) and Freundlich (dashed) isotherm models.

Freundlich Isotherm Model

Freundlich isotherm model is an exponential equation and assumes that the concentration of adsorbate on the adsorbent surface increases as the adsorbate concentration increases.

The model assumes that the adsorption could occur via multiple layers instead of a single layer.

Freundlich isotherm model writes:

$$q_e = K_F C_e^{\frac{1}{n_F}}$$

where K_F is the Freundlich equilibrium constant and n_F is the Freundlich exponent (dimensionless).

The larger the K_F value, the higher the adsorption capacity for a given adsorbate-adsorbent pair.

Sips Isotherm Model

Sip model, an empirical model, consists of the combination of the Langmuir and Freundlich isotherm models.

The Sips model:

$$q_e = \frac{Q_{max} K_S C_e^{\frac{1}{n_S}}}{1 + K_S C_e^{\frac{1}{n_S}}}$$

Where $0 < \frac{1}{n_S} < 1$.

K_S is the Sips equilibrium constant, Q_{max} is the Sips maximum adsorption capacity ($mg g^{-1}$), and n_S is the exponent.

At low adsorbate concentrations, Sips equation relatively reduces to the Freundlich isotherm, but it predicts a monolayer adsorption capacity characteristic of the Langmuir isotherm at high adsorbate concentrations.

Liu Isotherm Model

The Liu isotherm model is a combination of the Langmuir and Freundlich isotherm models, but the monolayer assumption of Langmuir model and the

infinite adsorption assumption that originates from the Freundlich model are discarded.

The Liu model predicts that the active sites of the adsorbent cannot possess the same energy. Therefore, the adsorbent may present active sites preferred by the adsorbate molecules for occupation, however, saturation of the active sites should occur unlike in the Freundlich isotherm model.

Liu isotherm writes:

$$q_e = \frac{Q_{max} K_g C_e^{n_L}}{1 + K_g C_e^{n_L}}$$

where K_g is the Liu equilibrium constant $(L\, mg^{-1})$; n_L is the dimensionless exponent of the Liu equation, and Q_{max} is the maximum adsorption capacity of the adsorbent $(mg\, g^{-1})$.

Contrary to the Sips isotherm, n_L could assume any positive value. [30]

3.3 Kinetic Adsorption Models

The adsorption kinetic models based on the chemical reaction such as pseudo-first order equation, pseudo-second order equation, n-general order equation Weber-Morris method will be discussed.

The pseudo-first-order and pseudo-second-order are the most commonly employed kinetic models for describing adsorption process based on chemical reactions kinetic, anyway the chemical reaction kinetic order depends upon the experimental data, sometimes a general-order is a better choice because different adsorption mechanism could concur simultaneously to the total adsorption.

Statistical parameters could be questioned to give an estimation of the good fitting of the model used with the experimental data.

$$\text{Reduced Chi-squared} = \sum_{i}^{n} \frac{\left(q_{i,\text{exp}} - q_{i,\text{model}}\right)^2}{n_\text{p} - p}$$

$$\text{SD} = \sqrt{\left(\frac{1}{n_\text{p} - p}\right) \cdot \sum_{i}^{n} \left(q_{i,\text{exp}} - q_{i,\text{model}}\right)^2}$$

$$R^2 = \left[\frac{\sum_i^{\text{np}} \left(q_{i,\text{exp}} - \bar{q}_\text{exp}\right)^2 - \sum_i^{\text{np}} \left(q_{i,\text{exp}} - q_{i,\text{model}}\right)^2}{\sum_i^{n} \left(q_{i,\text{exp}} - \bar{q}_\text{exp}\right)^2}\right]$$

$$R^2_\text{adj} = 1 - \left(1 - R^2\right) \cdot \left(\frac{n_\text{p} - 1}{n_\text{p} - p - 1}\right)$$

Figure 28: statistical parameters.

The lower the Reduced Chi-square and the standard deviation (SD), the lower the difference between the values of experimental adsorption capacity and theoretical one, therefore a best fitting is expected.

The R^2 and R^2_{adj}, are very useful parameters to evaluate if kinetic and equilibrium isotherm model fit well the experimental data. Their values are limited between 0 and 1, values of R_2 and R^2_{adj} closer to 1 means the model has a better fit.

The model with the best value of R^2_{adj} and the lowest value of SD should be considered as the best isotherm and kinetic model to describe the adsorption process. [30]

The pseudo-first-order equation

The simplest kinetic analysis of adsorption is the pseudo-first-order equation in the form:

$$\frac{\text{dq}}{\text{dt}} = \text{k}_\text{f}(\text{q}_\text{e} - \text{q}_\text{t})$$

Where q_t (mg/g) is the amount of adsorbate adsorbed at time t, q_e (mg/g) is the equilibrium adsorption capacity, K_f $(1/min)$ is the pseudo-first-order rate constant and t (min) is the contact time.

The integration of the above equation with initial conditions $q_t = 0$ at $t = 0$, and $q_t = q_t$ at $t = t$ leads to:

$$\ln(q_e - q_t) = \ln(q_e) - k_f t$$

That can be nonlinear rearranged to gives the equation known as pseudo-first-order kinetic adsorption equation:

$$q_t = q_e[1 - \exp(-k_f t)]$$

The pseudo-second-order equation

The pseudo-second-order is based upon equilibrium absorption capacity, this model assumes that the overall sorption rate is controlled by the rate of sorbate diffusion within the sorbent pores, it can be interpreted in terms of either ‘‘surface reaction’’ models, assuming that the transfer of sorbate across the solid/solution interface is the slowest step in the whole sorption process or the intraparticle diffusion model. [36]

The description of sorbate intraparticle diffusion into the porous particle is based on the Fick’s laws of diffusion.

The equation writes:

$$\frac{dq_t}{dt} = k_s(q_e - q_t)^2$$

where, k_s is the pseudo-second-order rate constant.

The integration of the above equation with initial conditions, $q_t = 0$ at $t = 0$, and $q_t = q_t$ at $t = t$ leads to:

$$q_t = \frac{k_s q_e^2 t}{1 + q_e k_s t}$$

This is the non-linear form of the model.

The adsorption times monitored in different experiments may differ by several orders of magnitude, depending on the physical nature of an adsorption system.

The general-order kinetic equation

Instead of the concentration of adsorbate in the bulk solution, now we pay our attention on the change in the effective number of active sites at the surface of adsorbent during adsorption.

The adsorption rate expression is given by:

$$\frac{dq}{dt} = k_N(q_e - q_t)^n$$

where k_N is the rate constant, q_e is the amount of adsorbate adsorbed by adsorbent at equilibrium, q_t is the amount of adsorbate adsorbed by adsorbent at a given time, t, and n is the order of adsorption with respect to the effective concentration of the adsorption active sites present on the surface of the adsorbent.

Theoretically, the exponent n can be an integer or non-integer rational number.

The number of the active sites (θ_t) available on the surface of adsorbent for adsorption can be defined as follow:

$$\theta_t = 1 - \frac{q_e}{q_t}$$

If an absorbent has not absorbed $\theta_t = 1$.

The value of θ_t decreases during adsorption process, it approaches a fixed value when adsorption process reaches equilibrium and $\theta_t = 0$ for a saturated adsorbent.

The rate of adsorption writes:

$$\frac{d\theta_t}{dt} = -k\theta_t^n$$

Where $k = k_N(q_e)^{n-1}$.

The integration of the absorption rate yields to the general-order kinetic absorption equation:

$$q_t = q_e - \frac{q_e}{[k_N\, q_e^{n-1}\, t\, (n-1) + 1]^{\frac{1}{1-n}}}$$

The first and second order kinetic equation are particular cases of the general-order kinetic equation for which $n = 1$ and $n = 2$.

3.4 CNTs adsorption mechanism

CNTs are 1D tubular open-ended materials and provide an external surface and hollow core for adsorption.

The International Union of Pure and Applied Chemistry (IUPAC) provides a useful classification of pores according to their diameter:

- micropores, size less than 2nm
- mesopores, size between 2nm and 50nm
- macropores, size more than 50nm

In MWCNTs the nature of the porous can be classified as inner hollow cavities of small diameter (ranging from 3 to 6 nm in a narrow distribution of sizes) and aggregated pores (widely distributed, 20–40 nm), formed by interaction between the CNTs. The aggregated pores are formed by entanglement of several MWCNTs, which are adhered to each other as a result of van der Waals forces.

Many methods of characterization have shown the microporous preferable nature of SWCNTs and the mesoporous preferable nature of MWCNT. [29]

SWCNTs usually exhibits a specific surface area (SSA) bigger than MWCNTs.

The SSA of macroscopic samples of powders or porous materials is routinely determined by measurement of gas adsorption (generally N at 77 K) and calculated using the Brunauer–Emmett–Teller (BET) isotherm.

A. Peigney et al. geometrically derive the external SSA of CNTs bundles as a function of the number of nanotubes that compose the bundle, the number of shell and the diameter of the tubes, they found a very broad scale, from 50 to 1315 m^2/g, decreasing the number of tubes. [37]

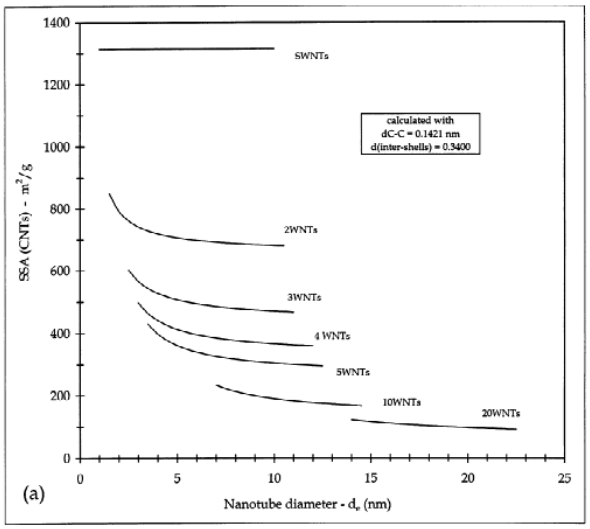

Figure 29: SSA as a function of number of shell and diameter.

For SWCNT, the diameter of the tubes and the number of tubes in the bundle will affect mainly the textural properties values, since in bundle the adsorption sites are different to those expected for an individual nanotube.

the adsorption on SWCNT bundle can occur at four different sites:

- the grooves formed at the contact between adjacent tubes
- outside of the bundles
- the interstitial channels between the tubes in bundles
- inside of the nanotubes (pores) with open ends

In contrast to the SWCNT, the MWCNTs are not in the bundles form and their adsorption sites consist of pores aggregated in the inner MWCNT surface with open ends and on the outer walls, also the presence of defects should be considered as reactive sites for adsorption.

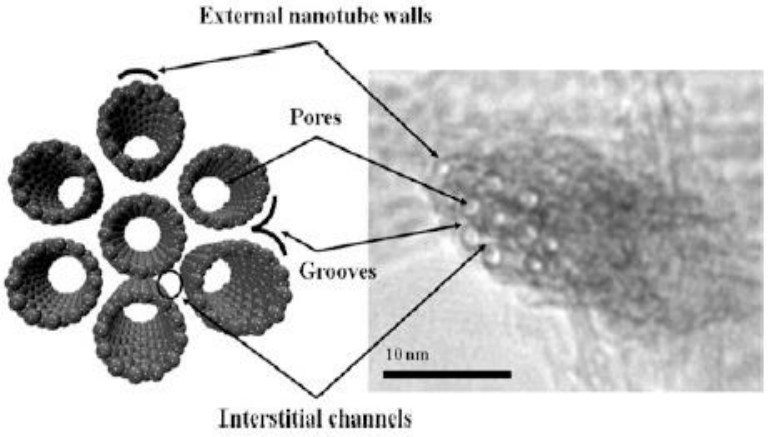

Figure 30: Adsorption sites of SWCNT bundle and TEM.

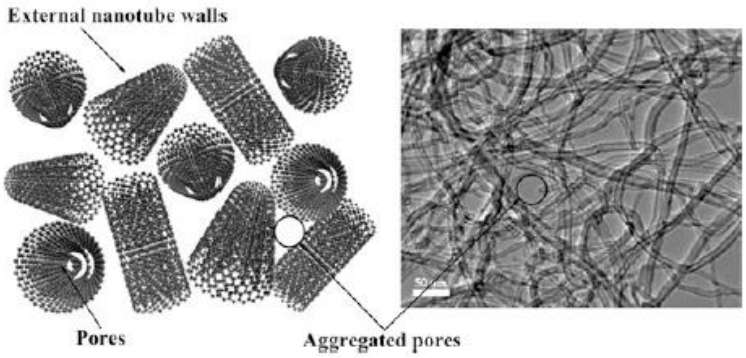

Figure 31: Pores aggregated of MWCNT and TEM.

In particular, when considering surface properties, the benzenoid rings of CNTs have high polarity resulting in a hydrophobic material and favours the high efficiency adsorption of hydrocarbons and aromatic compounds by π–π coupling stacking. [38]

Furthermore, the CNT structure permits the incorporation of one or more chemical functional groups such as a hydroxyl group (–OH), carbonyl group (–C=O), or carboxylic group (–COOH) which may increase the selectivity and the stability of the resulting system.

Functional groups may change the wettability of CNT surfaces, producing more hydrophilic CNTs that enhance the adsorption of lower molecular weight and polar compounds. [38]

The chemical functional groups may be anchored to the CNT surface through functionalization or purification processes that can significantly alter the textural properties of CNTs. They increase or decrease the specific surface area, total volume pore, or even resulting in the modification of the chemical surface of these nanostructures.

Heat treatment can be done to reverse the process and remove the functional groups.

Moderate oxidation of CNTs using acids such as sulfuric acid (H_2SO_4) and nitric acid (HNO_3) increases their capability to adsorb aromatic compounds through π–π interactions, however, strong oxidations lead to amorphous carbon formation, which is deleterious for availability of sites for π–π interactions.

A great advantages of CNTs is their quick regeneration from pollutants without losing its adsorption capacity. [39] Regeneration can be provided by the use of solvent such acetone, that open the pores of CNTs and inactivates the adsorption sites.

The phenomenon of Adsorption/desorption hysteresis was also observed for small molecules, it is presented as deviation of desorption curves from adsorption ones.

Organic compound adsorption

Numerous studies have already investigated the role of CNTs as effective adsorbents for organic chemicals compared with C_{18} and activated carbon (AC) performances. [40]

Tao Liu et al. studied the adsorption capacity of MWCNTs on adsorption of oily substances such as gasoline, kerosene and diesel. They evidence that the adsorption capacity decreases after the firsts cycle of adsorption/regeneration, finding a stabilized adsorption capacity around 5 g/g of CNTs for gasoline and kerosene and around 8 g/g of CNTs for diesel, the great performance of adsorption for these substances is justified by the hydrophobic and oleophilic nature of carbon nanotubes. [41]

Organic chemical adsorption on CNTs could not be described using a single adsorption coefficient due to the heterogeneity of the adsorption mechanism.

The structural properties of CNT allow a strong interaction with organic molecules through noncovalent forces such as hydrogen bonding, electrostatic forces and van der Waals forces.

Organic chemicals may occupy high-energy adsorption sites first, and then spread to sites with lower energy, this hypothesis could indicate concentration-dependent thermodynamics and kinetics.

The dominant adsorption mechanism is different for different types of organic chemicals (such as polar and nonpolar), thus different models may be needed to predict organic chemical-CNT interaction, the sorption equilibrium data are mostly related either with the Langmuir or the Freundlich equations (or both) tried to find a link between empirical isotherms and heterogeneity of the surfaces. [41]

Multilayer adsorption could occur when organic chemicals were adsorbed on CNT surfaces, in this process, the first couple of layers interact with the surface, while molecules beyond the first two layers interact with each other. This process is called surface condensation, the energy of this process varies depending on the distance between the adsorbed molecules and the CNT surface, thus causing a distribution of adsorption energy. [42]

Metallic ions adsorption

For metallic ions, the parameters such as pH and temperature play a fundamental role in CNTs sorption.

An increment in temperature increases the amount of metal ions adsorbed, and it reduces the time to obtain 50 % of maximum sorption capacity.

In this regard, the sorption mechanism is attributable to chemical interaction between the metallic ions and the surface functional groups.

In addition, adsorption of metallic ions on CNTs may involve other complex mechanisms such as electrostatic attraction and precipitation.

Marko Šolic' et al. prove that adsorption of Cu(II) and Ni(II) is largely driven by electrostatic interactions and surface complexation at the interface of the adsorbate/adsorbent system. [43]

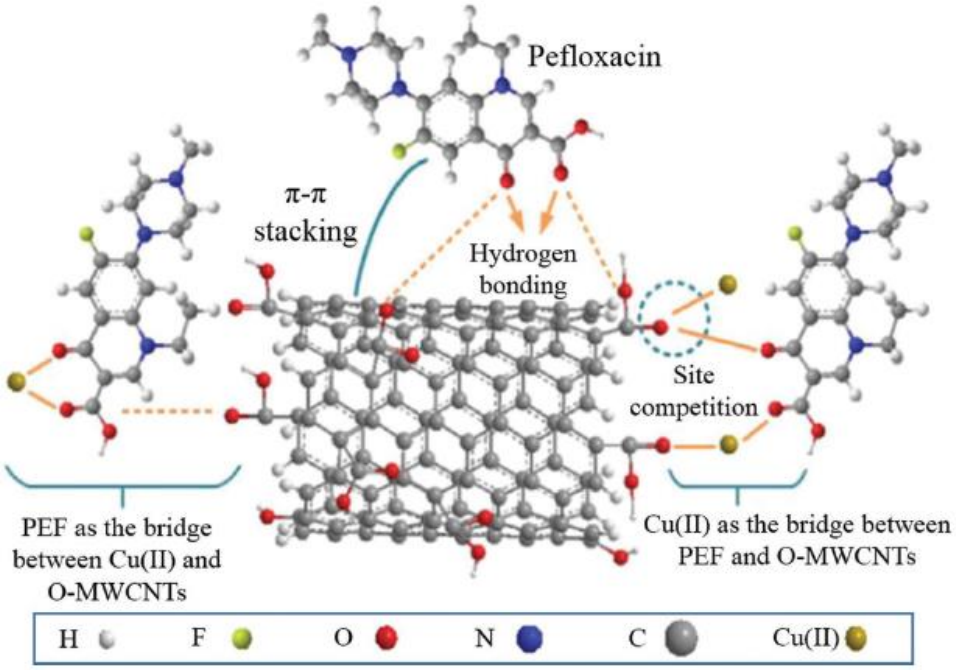

Figure 32: mechanism for co-adsorption of Cu(II) and PEF on oxydic MWCNTs (O-MWCNTs)

4 Materials and methods

In order to investigate the possibility to use Innovacarbon material as swimming pool water filter material, different solutions with contaminants typically present in the water of swimming pools have been prepared to simulate a possible polluted situation.

Three substances have been considered:

- Ammonia
- Urea
- Solar oil

The analysis of each of them have bring some experimental issues, so it has been impossible to standardize the methods of analysis, different approaches for each substance were used to check if they could be absorbed by the Innovacarbon material.

4.1 Innovacarbon material

The material produced by Innovacarbon SRL essentially consists of Multi-Walled Carbon Nanotubes anchored on a quartzite sand, Supported Multi-Walled Carbon Nanotubes (SMWCNTs)

The carbon nanotubes are synthetized by a CVD process, using Fe-Co as catalyst, in a reactor made of quartz with a process temperature of about 700°C and ethylene as a carbon source.

The process has been optimized to produce large quantities of MWCNTs characterized by an important quantity of structural defects, this enhances the number of different possible adsorption sites.

The quartzite sand is the same used in commercially sand filters, with diameter ranging from 500 to 800 micrometres, it behaves as substrate for the CVD growth of the nanotubes and must not be removed after the synthesis but is itself part of the final product.

Subsequently the CVD stage, the material is sieved to eliminate the CNTs dust that has not adhered well to the support.

Figure 33: CVD reactor at Innovacarbon srl production site.

The Multi-Walled Carbon Nanotubes as produced are characterize by an average of 8 walls (TEM), a medium length of 20 µm (SEM-TEM) and external diameter of 18 nm (TEM). The amorphous carbon present is less than 1%wt. (Tga-DTA).

The density of the material is of 1500 kg/m^3, it is insoluble in water and thermal decompose at around 550 °C producing carbon.

The means weight corresponding to carbon nanotubes with respect to the full weight of the material is calculated to be the 2,5%, so for each gram of material there are 0,025 g of CNTs.

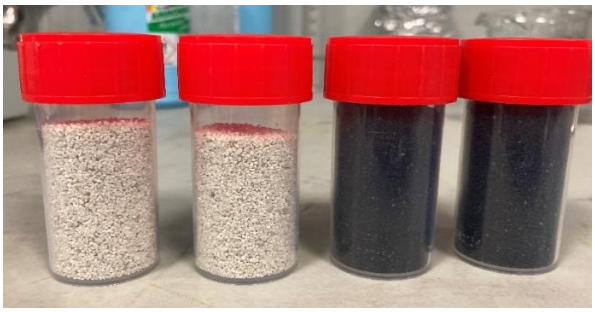

Figure 34: Quartzite sand and Innovacarbon material.

Thanks to the support of the laboratory of Politecnico di Milano has been possible to characterize the material with Raman spectroscopy.

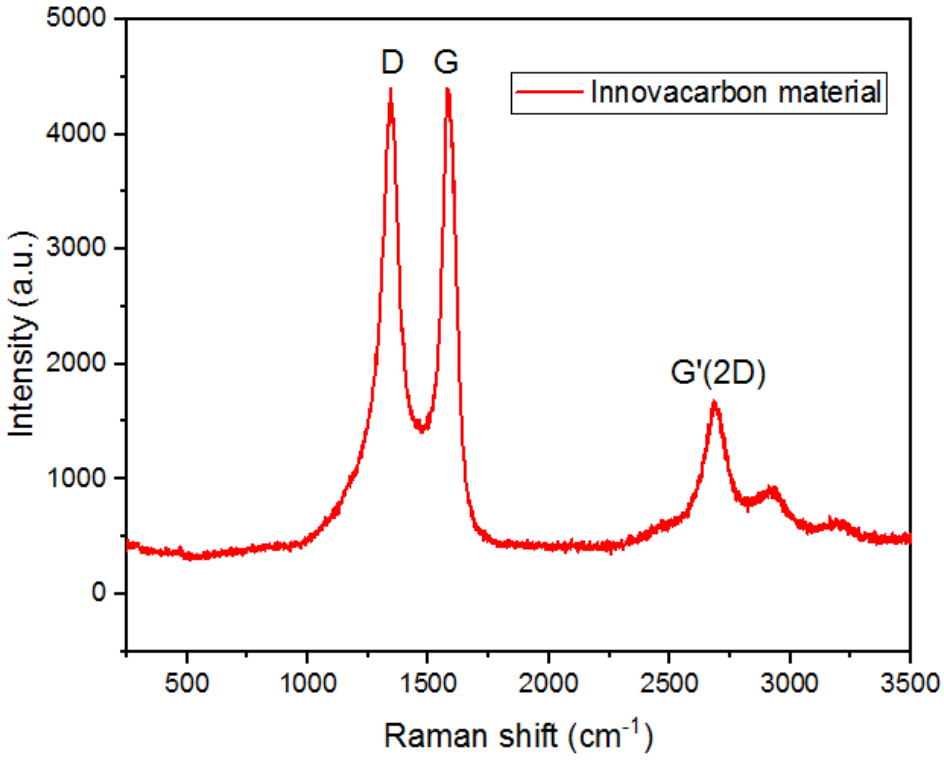

Figure 35: Raman spectra of Innovacarbon material.

From the Raman spectra is possible to distinguish the two typical peak of MWCNTs.

The D peak at around 1350 cm^{-1} related to the disorder of the structure.

The G peak at around 1580 cm^{-1} related to the graphitic structure of the CNTs.

The fact that the two peak have almost the same intensity indicates the large presence of defects in the structure, these defects in the case of application of nanotubes in adsorption processes are not a negative features, while are additional active sites for interactions.

4.2 Laboratory scale filter system

To provide the laboratory tests, a reproduction in scale of a real filter has been constructed, the system work as an absorption column.

A peristaltic pump has been used to simulate the behaviour of pump system of a filter, the model of the pump is VWR SP100, it has 99 different velocities and can work in direct or reverse flux.

The core of the absorption column consists of millimeter dropper with an open/closed valve, with the addition of two glass connector, one for the input and one for the output, in which a 50 cm Tygon® tubes are stuck to permit from the side below to bring the polluted water from a backer, passing troughs the pump and arrive to the dropper and to the other side, positioned above, to let go out the processed water.

Dropper of 50 ml, 100 ml and 250 ml have been employed depending on the application and quantity of material needed for the peculiar experiment. Inside the dropper is placed the Innovacarbon material and two sink filter of grid dimension less than 500 micrometres are stuck one below and one in the upper part to ensure that the sandy material is not dragged by the passage of water.

If the experiment is developed in continuous, one backer contains the initial solution and another free backer is used to store the treated water. If a closed-circuit experiment is done, the same backer is used as input and output.

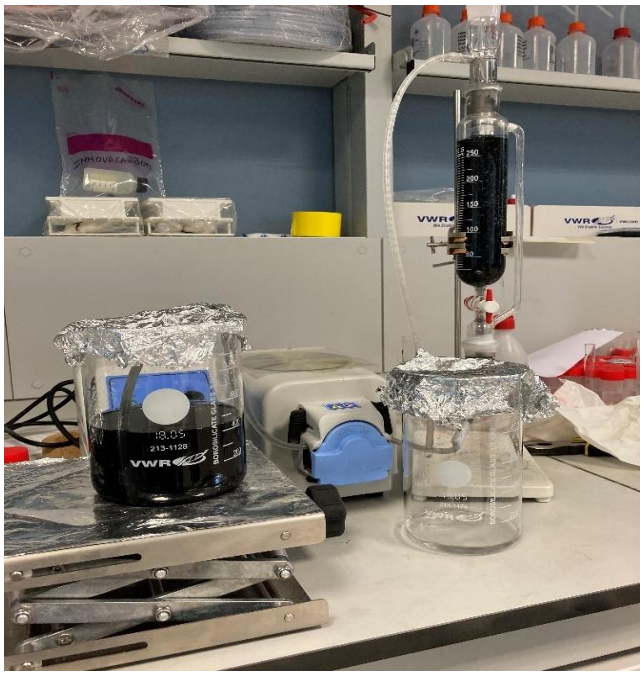

Figure 36: Laboratory filter system during an experiments on colorants.

4.3 Regeneration system

After the process of filtration has finished it is possible to regenerate the material.

The absorption column is disassembled, and a solvent is made to pass by gravity through the material remained in the column, it can open the pores and disactivate the bonds created between the pollutant and the carbon nanotubes in order to release the trapped substances.

Pure Acetone is used for this scope, in a relation 2/2,5 ml of acetone for each g of material, this quantity can vary depending on the water treated.

Later, to reactivate the nanotubes, 2,5 ml of water for each g of materials is made pass through the column, this quantity of water permits a very low (uninfluential) residual of acetone in the column.

The material can then be heated at 130°C for some hours to let the humidity evaporates, the material is utilizable other times without having a loss of performance. This has been verified also for other applications, and it has been considered as hypothesis of this work.

This last, passage is not mandatory because the material could be used also if it is not dry at the beginning of the experiments, in this case could be important to consider the quantity of water stored in the column during the subsequent measure.

The dirty Acetone is recovered by distillation with VWR®LED Digital Rotary Evaporator, the operational conditions are:

- 65 °C
- 50 rpm
- Velocity 50 of the peristaltic pump

In one hour, it is possible to recover more or less 500 ml of Acetone, with yield 95/98 %, the system could be more efficient if combined with a vacuum pump.

Sometimes it is possible to recover the pollutant, if it is something reusable such as polyphenol, petroleum, colorants dye etc. or if it is not, such in the case of swimming pool contaminants, it will be disposed.

Figure 37: Rotary Evaporator.

4.4 Contaminants

As contaminants have been analysed three different substances that are commonly present in polluted swimming pool water, Ammonia and Urea can be released directly from the human body, solar oil could be transported into the pool by the bathers.

All the solution contains the pollutant and mineral water as solvent taken from the tap, as in swimming pool the water is also provided by the city hydraulic system.

Ammonia

For ammonia, three solution with known concentration,

- 30 mg/L
- 87 mg/L
- 126 mg/L

were used to correlate the ammonia concentration with the intensity of absorption in UV-Vis spectra, derived from the coloration methods.

The solutions were available in neutral and pH 2 form, both were analysed, and the medium of the results was considered.

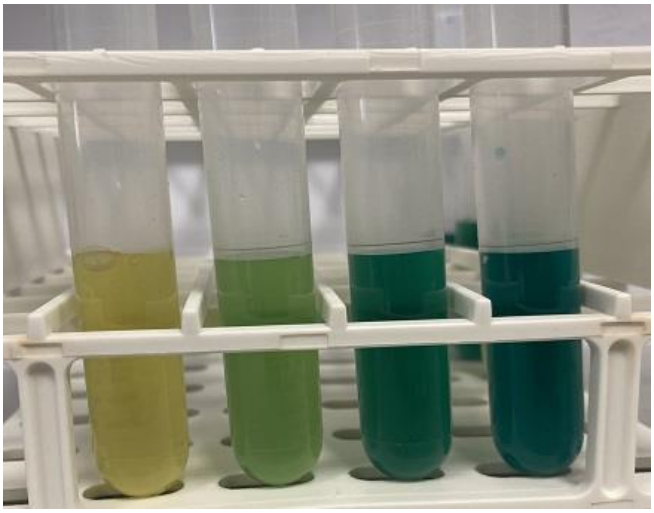

Figure 38: Ammonia concentration of 0 mg/l, 30 mg/l, 87 mg/l, 126 mg/l after Spectroquant® ammonium test coloration.

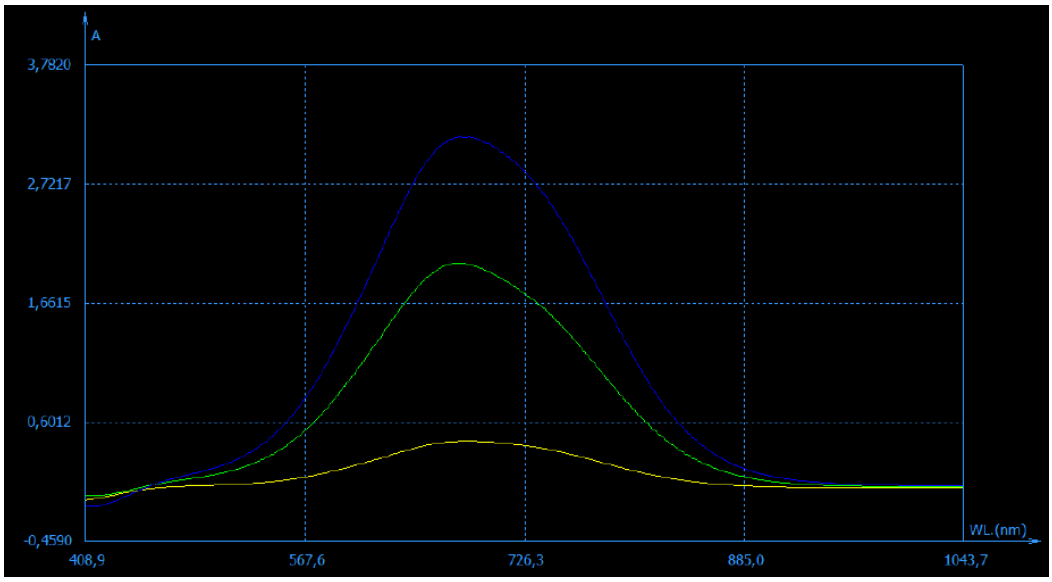

Figure 39: Ammonia standard curves with UV-Vis spectrophotometer.

The peak of absorption was found to be around 682 nm (green colour), a linear fitting interpolation (y = a + b*x), using the program 'Origin pro 2019b' was done

to obtain the parameters necessary to provide quantitative analysis of the treated samples.

The resulting parameters are reported in the table below.

Intercept (a)	Slope (b)	Adj. R-Square
-0,14529	0,02694	0,98125

Table 2: Linear fitting parameters for ammonia.

Urea

Urea solution has been created starting from pure solid Urea manufactured by VWR Chemicals.

Different quantities of Urea have been mixed with water to create solutions with two different concentration:

- 140 mg/L
- 200 mg/L

Of course, these are very high as very improbable concentration to find in a swimming pool, but it has been necessary to use such concentrations due to the limitations imposed by the instruments of analysis.

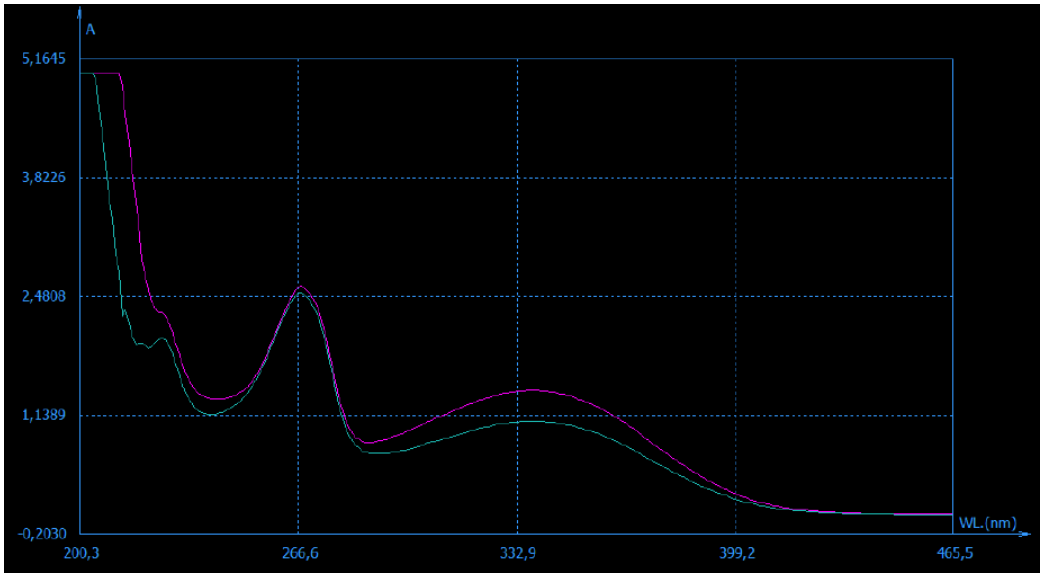

Figure 40: Urea standard curves with UV-Vis spectrophotometer.

From the analysis of the UV-Vis spectra it has been possible to identify a peak at 338 nm that has been associate to the presence of nitrogen, and so of urea in water after the treatment with Spectroquant® Nitrogen (total) Cell Test.

From the data of absorption at that wavelength and knowing the concentrations, a linear fit (y = a + b*x) has been done, providing the following parameters.

Intercept (a)	Slope (b)	Adj. R-Square
0,01487	0,00719	0,99289

Table 3: Linear fitting parameters for urea.

Solar oil

Due to the impossibility to test all the different kind of solar oil and solar cream, a generic solar oil has been taken for the study.

The oil used is 'Conad Essentiae' with ingredients: Paraffinum liquidum, Dicaprylyl Ether, Butylene Glycol Dicaprylate/Dicaprate, Ethylhexyl Cocoate,Dycapryltl Carbonate, Butyl Methaoxydibenzoylmethane, Octocrylene, Caprylic/Capric Triglyceride, Simmondsia Chinensis Seed Oil, Theobroma Cacao Extract, Parfum, Ethylhexyl Triazone, Lecithin, Tocopheryl Acetate, Tocopherol, Ascorbyl Palmitate, Citric acid, Eugenol.

These substances have typically organic nature, usually founded in cosmetic products.

Due to the immiscibility of the oil with water it has been very difficult to analyse it with the UV-Vis spectrophotometer, to resolve this problem an extraction process it has been done with use of n-heptane as extractor.

The prepared solution of water/solar oil has been stirred for ten minutes at 600 rpm, then 10 ml of solution was pipetted in a sample, and 10 ml of heptane was added there, due to a difference in density it was possible to clearly see the separation of phases between water and heptane.

To provide the extraction of the solar oil from the water to the heptane, in which it results miscible, other 20 minutes of stirring at 600 rpm has been done, followed by 20 minutes of relaxing.

Finally, 4 ml of the above solution (heptane/solar oil) has been pipetted in a cuvette and then measured with the spectrophotometer, using pure n-heptane as blank.

This process was repeated for prepared solution water/solar oil with different concentration:

- 31,25 mg/l
- 62,5 mg/l
- 125 mg/l
- 250 mg/l
- 500 mg/l
- 1000 mg/l

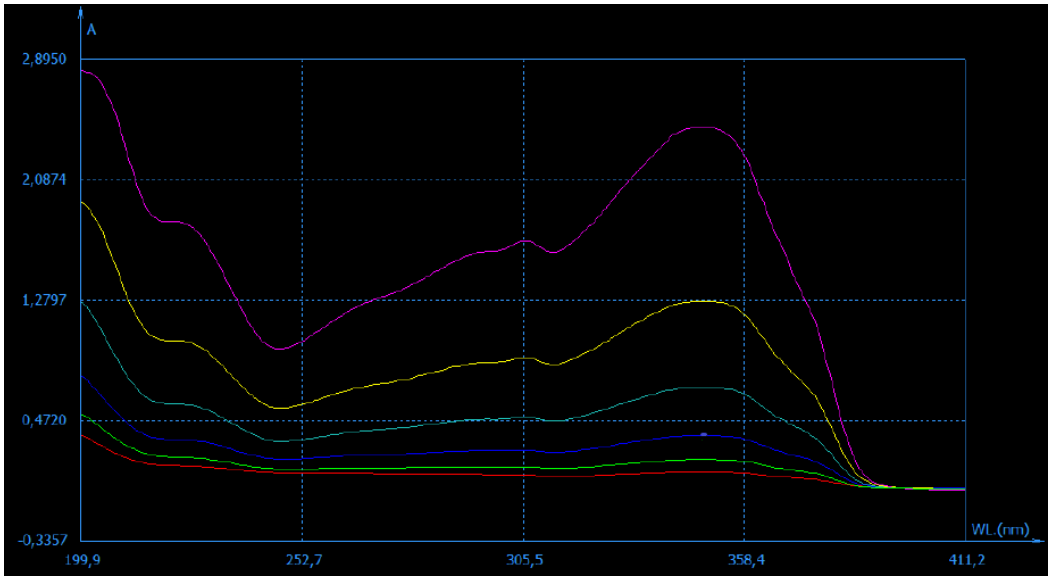

Figure 41: Solar oil standard curves with UV-Vis spectrophotometer.

It is impossible with the spectrophotometer to recognize each substance, but it has been possible to identify three peaks that have been associated to different classes of compounds.

The peak at around 305 nm and 348 nm have been associated to the oily substances, while the peak at 230 nm to the additives.

From the known data of adsorption and concentration a linear fit (y = a + b*x) has been done, providing the following parameters.

Intercept (a)	Slope (b)	Adj. R-Square
0,05346	0,00241	0,99859

Table 4: Linear fitting parameters for solar oil.

The Adj. R-Square (0,99859) is very close to 1, it guarantees a good fitting of the data making possible accurate quantitative analysis.

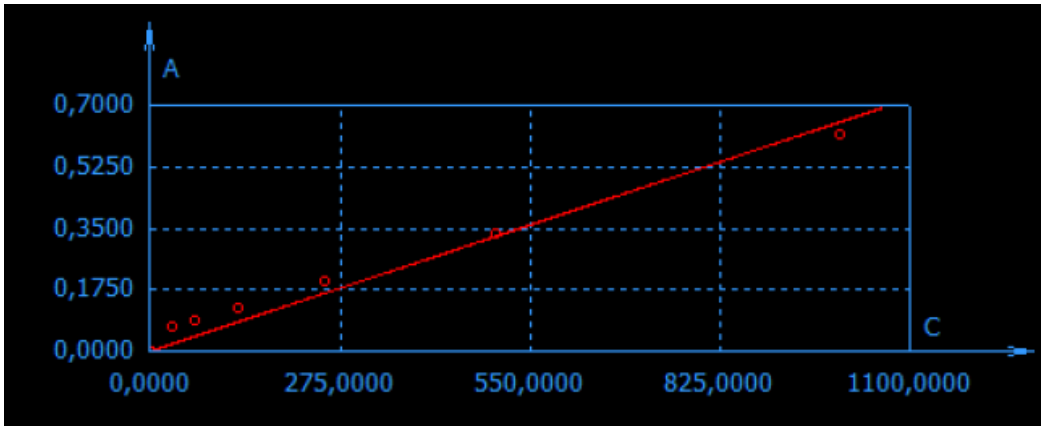

Figure 42: Linear fitting of different concentration of solar oil.

Figure 43: Ammonia, Urea, Solar oil.

4.5 UV-VIS spectrophotometer

The spectrophotometer used for the whole spectra analysis is the UV-1600PC Spectrophotometer produced by VWR.

The scanning range go from 199 nm to 1200 nm with a scan interval imposed at 1 nm, the spectrophotometer uses two lamp (W lamp, D2 lamp) to run along the whole range of wavelength.

The spectrum can be display both in wavelength-transmittance and wavelength-absorbance.

Figure 44: UV-Vis spectrophotometer by VWR.

Molecules containing bonding and non-bonding electrons (n-electrons) can absorb energy in the form of ultraviolet or visible light to excite these electrons to higher anti-bonding molecular orbitals, the more easily the electrons can be excited (lower energy gap between the HOMO and the LUMO), the longer the wavelength of light it can absorb.

Lambert-Beer law's governs the process of wavelength-absorption, it states that the absorbance of a solution is directly proportional to the concentration of the absorbing species in the solution and the path length.

$$A = log_{10}\left(\frac{I_0}{I}\right) = \epsilon c L$$

where A is the measure of absorbance (in Absorbance Units (AU)), I_0 is the intensity of the incident light at a given wavelength, I is the transmitted intensity, L the path length through the sample, c the concentration of the absorbing species and ϵ the extinction coefficient that vary for each substance and also depends on the interaction with the solvent, it can be extrapolate with a calibration curve for each combination of substance-solvent.

At sufficiently high concentrations, the absorption bands will saturate and show absorption flattening, this is due to the fact that close to 100% of the light is already being absorbed. The concentration at which this occurs depends on the particular compound being measured, giving an absorption intensity of 5 a.u.

The samples are prepared in a 10 mm quartz cuvette and as blank has been used tap water, not distilled one, because the samples are prepared with the same water, and also swimming pool are not filled with distilled water.

4.6 Ammonia and urea tester

To be able to analyse the ammonia and the urea with the UV-Vis spectrophotometer it has been necessary to use two different tester as simply with the spectrophotometer was impossible to identify the peak of these substances.

Spectroquant® Ammonium Test

In strongly alkaline solution ammonium nitrogen is present almost entirely as ammonia, which reacts with hypochlorite ions to form monochloramine.

This in turn reacts with a substituted phenol to form a blue indophenol derivative that is determined photometrically.

Due to the intrinsic yellow coloration of the reagent blank, the measurement solution is yellow-green to green colour.

The method is analogous to EPA 350.1, APHA 4500-NH_3 F, ISO 7150-1, and DIN 38406-5.

The measuring range for a cell of 10 mm is 2.0-150 mg/L NH_4-N and 2.6-193 mg/L NH_4^+ for a maximum of 100 determinations.

The test measures both ammonium ions and dissolved ammonia, it is idoneous to analyses groundwater and surface water, seawater, drinking water, wastewater, nutrient solutions for fertilization, soils and food after appropriate sample pre-treatment.

The procedure is not complicated:

- Pipette into a test tube 5,0 ml of Reagent NH_4-1
- Add 0,1 ml of the sample with a pipette and mix
- Add 1 level blue microspoon of Reagent NH_4-2 and shake vigorously until the reagent is completely dissolved

After a reaction time of 15 min, a 10 mm cell is filled with the sample and measured in the photometer.

Spectroquant® Nitrogen (total) Cell Test

Organic and inorganic nitrogen compounds are transformed into nitrate according to Koroleff's method by treatment with an oxidizing agent in a thermoreactor.

In a solution acidified with sulfuric and phosphoric acid, this nitrate reacts with 2,6-dimethylphenol (DMP) to form 4-nitro-2,6-dimethylphenol that is determined photometrically.

The digestion is analogous to EN ISO 11905-1.

The determination of nitrate is analogous to DIN 38405-9.

The measuring range is 10-150mg/l N for 25 determinations.

The test is idoneous to analyses groundwater and surface water, drinking water, wastewater, industrial water, nutrient solutions for fertilization, soils and food after appropriate sample pre-treatment.

It is not suited for seawater.

Procedure:

- Pipette into an empty cell 1,0 ml of the sample to be analysed
- Add 9,0 ml of distilled water and mix
- Add 1 level blue microspoon of Reagent N-1K and mix
- Add 6 drops of Reagent N-2K, close the cell and mix
- The cell must be heated at 120°C in the preheated thermoreactor for 1 h, the digestion process occurs.
- Cool down without cold water for 10 minutes and shake the cell
- Pipette into a reaction cell 1,0 ml of the digested, cooled sample
- Add with pipette 1,0 ml of Reagent N-3K, close the cell tightly, and mix.
- Wait 10 minutes (reaction time).

Finally, it is possible to measure the sample with the spectrophotometer.

Unlike with Spectroquant® ammonium test, a colour change does not occur in this case.

4.7 Experiments

Two different kind of experiments have been done to obtain the data required for further considerations: kinetic experiments and treatment experiments.

The kinetic adsorption tests have been important to try to identify the mechanism of adsorption of carbon nanotubes, in particular, the form synthetized by Innovacarbon srl.

The treatment experiments tested the operation of Innovacarbon material in the adsorption column that simulate a filter system for swimming pool.

All the experiments were realized at constant temperature of 25 °C and the pH of solution was not considered as a parameters.

For all the experiments it has been used material that was previously employed for other applications and then regenerated, it has been verified and taken as important hypothesis that the material in general does not change its adsorption capacity after multiple uses.

4.7.1 Kinetics

The kinetics experiments have not been developed in batch, differently from what had been done in most kinetic studies for absorbent materials, but directly in the adsorption column, due to the impossibility of stirring the material.

In fact, the friction between the grains of sand that would be created with the rotation may cause many carbon nanotubes to detach from the support, changing the nature of the adsorbent material.

The kinetic experiment was done for CNTs/ammonia and CNTs/solar oil systems.

The procedure of the experiments was standardized as much as possible.

An absorption column has been filled with 80 g of material and 40 ml of solution is passed through the column by gravity, these quantities permit to almost wet all the volume of the material without or with a very few quantity of solution that remain above the material and so untreated, but this is not a problem, because not all the volume of treated solution can be further collect, due to the wettability of the material, some millilitres of polluted water remain trapped in the column.

One times all the volume of the material has been wet, the timer starts, and samples are taken at specific time. The contact times considered were 10 sec, 30 sec, 1 min, 5 min, 30 min, 1 h, 2 h.

For each time, new but not pristine material has been used, so after each test, the material get regenerate.

Ammonia kinetic experiment

The kinetics studies on ammonia have been done on two prepared solution with commercial ammonia and tap water, in 500 ml of volume of water, the analysis of these solution with the UV-Vis spectra bring to initial concentrations of:

- 33 mg/l
- 49mg/l

Using these concentrations as starting point reduces the error, due to the fact that the concentration of commercial ammonia is not so accurate.

The treated sample taken at each time were subsequently processed with the Spectroquant® Ammonium Test in order to be able to analyse it with the spectrophotometer.

The results were subsequently analysed with 'Origin Pro 2019b'.

In the figure below an example of the samples after the coloration with the Spectroquant® Ammonium Test. The yellow one is the blank sample, in which no ammonia is present. The green one is the 33 mg/l sample before the treatment, while the light green are the treated sample at 10 sec and 5 min.

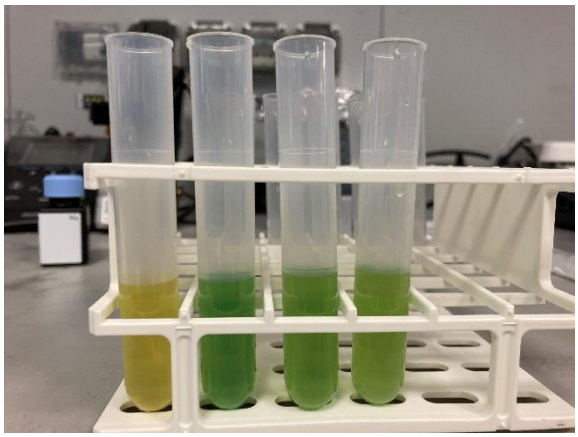

Figure 45: Spectroquant® Ammonium Test (blank, 33 mg/l, 10 sec, 5 min).

Solar oil kinetic experiment

The kinetic studies on Solar oil have been done preparing different solution using solar oil 'Conad Essentiae' and tap water, 50 mg, 200 mg and 1000 mg was weighted with a precision balance and mixed with a volume of water of 500 ml. Resulting in theoretical concentration of:

- 100 mg/l
- 400 mg/l
- 2000 mg/l

Due to the immiscibility of the two substances, a magnetic agitator is used to continuously stirring the volume at 600 rpm, to try to homogenize as much as possible the solution.

In general, treating this substance brings an intrinsic error, due to the fact that some of the oily solution can adheres to the surface of the glass of the beaker, and so bring to lower analysed concentrations.

So, for the elaboration of the data will not be used the prepared concentration as initial concentration, but the concentrations measured with the UV-vis spectrophotometer after extraction with heptane, to not overestimates the adsorption capacity of the material.

So as starting concentration are considered:

- 45 mg/l
- 204 mg/l
- 878 mg/l

At each testing time 10 ml of treated solution was collected in a sample and then 10 ml of heptane was added to the sample to proceed with extraction of the oily part left in solution.

The extraction process consists of 20 minutes of stirring at 300 rpm and 20 minutes of relax of the solution heptane/oil, the residual solution was tested with the spectrophotometer, using pure heptane as blank, to quantify the residual concentration of solar oil in solution.

4.7.2 Close circuit treatment

To have a more realistic idea about the workability of the filter system for swimming pool, simulation of close circuit treatment has been done for ammonia, urea and solar oil.

A beaker has been filled with polluted solution, simulating a contaminated swimming pool, then the water recirculates through the filter in the beaker.

Different samples were taken from the pool at different times.

Ammonia

A solution with concentration of 25 mg/l has been prepared, using 250 ml of water.

The absorption column has been filled with 150 g of material, that corresponds to 3,75 g of Carbon nanotubes, the system work thanks to a peristaltic pump as described in the previous chapter.

The polluted solution enters the filter from beyond, this is done because in this way the probability for the solution to takes preferential via inside the core of the material is reduced and the mobile front can be better controlled.

It is also possible too better control the throughput, the velocity of the pump has been fixed at 10, that in this case corresponds to around 15 ml/min, so every 20 minutes more or less all the volume of solution could be treated.

Sample of the treated solution was processed with Spectroquant® Ammonium Test and then analysed with UV-Vis spectrophotometer at different times: 20 min, 40 min, 1 h, 2 h, 4 h.

Urea

As for ammonia the same treatment has been done for urea, first, 70 mg of urea has been weighted with a precision laboratory balance with sensibility 0,01 g, then 100 mg, in a volume of water of 500 ml.

Two solution with different concentration was obtained:

- 140 mg/l
- 200 mg/l

This time 80 g of material and 250 ml of solution was employed, the velocity of the pump was fixed at 10 with a resulting throughput of 25 ml/min, samples at different times were taken: 2 min, 10 min, 30 min, 2 h, 5 h.

The sample were treated with Spectroquant® Nitrogen (total) Cell Test and then analysed with the UV-Vis spectrophotometer. The results were processed with the support of 'Origin Pro 2019b'.

Solar oil

To simulate the filtration system with solar oil, a lot of inconvenient has been encountered, it was not possible to use the pump because most of the oil adheres to the walls of the tube, furthermore due to immiscibility and the tendency of floating of the oil, also trying to take the water from the free surface brings a lot of inconvenient in the attempt to collect all the oily parts.

The solution has been stirred for 10 minutes at 600 rpm and then overturned from above in the adsorption column, without using the pump to provide the circulation of the solution, the throughput is governed by the gravity, giving as result 125 ml/min.

With two beaker has been created a fictitious close circuit, in this case all the volume is treated in each round.

Samples of treated solution have been analysed after 1 round and 2 rounds.

While for ammonia and urea were possible to verify the maximum absorption capacity during the close circuit treatment or the kinetics experiment, as a total elimination of the pollutant was never achieved.

For solar oil during the kinetic experiments or the close circuit treatment, almost all the pollutant has been adsorbed by the material, so, results necessary to force more the material to evaluates its maximum adsorption capacity.

For this purpose, 500 ml of the solution with concentration 12 g/l has been prepared and treated with a decrescent amount of material, in this way was possible to find the limits of adsorption of the material.

It was impossible to measure such a big concentration with UV-vis spectrophotometer, due to overflow of the signal (more than 5 a.u. of intensity). From the spectra taken during the kinetic experiments, it was noticed that usually the result from the spectra gives a concentration inferior with respect to

the prepared one, due to losses of solar oil attached to the wall of the glass. So, to not overvalued the results, it is considered as initial concentration that really could be get in contact with CNTs a value reduced from 12 g/l to 10 g/l.

The first time 160 g of material was used, with an height of the column of 11,5 cm and the data was collected after 1 round and 2 round, because a negligible quantity of solar oil remained in solution.

The same was done with 120 g of material, height of the column of 8,5 cm.

A final attempt was done with 80 g of material and height of the column of 6 cm, with samples analysed at 1 round, 2 rounds, 5 rounds, 10 rounds, 15 rounds. With this configuration was possible to obtain the desired result.

5 Discussion of results

The analysis of the data obtained by the different experiments permits interesting considerations, the intrinsic differences between the pollutants considered permits to better understand the interaction of carbon nanotubes with different type of molecules.

In order to better compare the obtained results with other carbonaceous adsorbent materials, all the adsorption capacity will be refereed to just the adsorbent part of the material (carbon nanotubes) and not to the total weight of the material. The 2,5 %wt. of the total weight corresponds to carbon nanotubes, so the result of adsorption capacity will be expressed in terms of mg/g_{CNTs}.

Before analysing the results, it could be better to expose the hypothesis taken into consideration in this work:

- The mean content of carbon nanotubes in the material is constant and equal to 2,5 %wt.
- Temperature and pH are not considered as parameters, all the experiments are provided at 25°C.
- The behaviour of the material is independent of the initial concentration of the pollutant, especially for very low concentrations.
- The system is scalable without losing of generality.
- The filter with Innovacarbon material work at least as a traditional sand filter for what concern adsorption of molecules bigger than 100 µm.

5.1 kinetic model

From the kinetic experiments have been possible to adapt kinetic model of adsorption for the interaction CNTs/solar oil and CNTs/ammonia.

Kinetic model of adsorption for CNTs/ammonia system

Pseudo-first order and pseudo-second order model were used to interpolate the data obtained from the experiments of adsorption of ammonia by carbon nanotubes, the visual results are present in the graphs below for initial concentration of ammonia of 33 mg/l and 49 mg/l.

It was not possible to fit the data with the general-order kinetic model due to a too sudden change of slope of the experimental data, producing a divergent result.

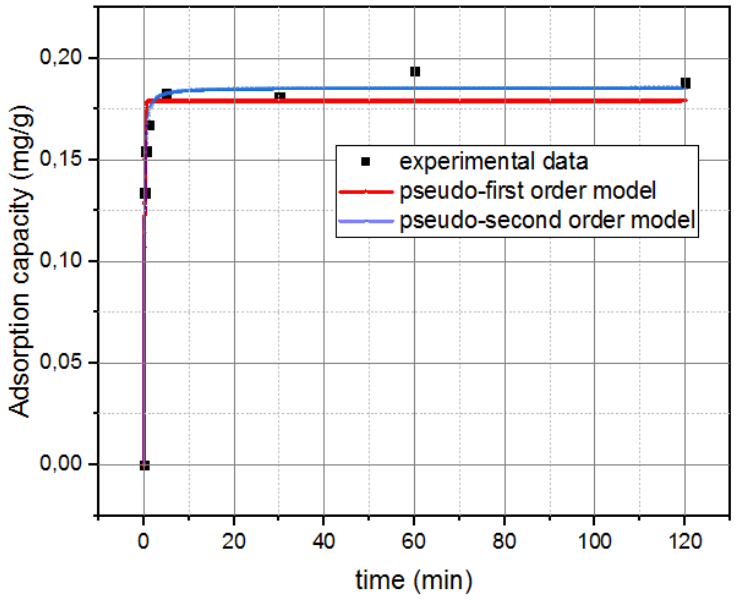

Figure 46: Kinetic model for ammonia initial concentration of 33 mg/l.

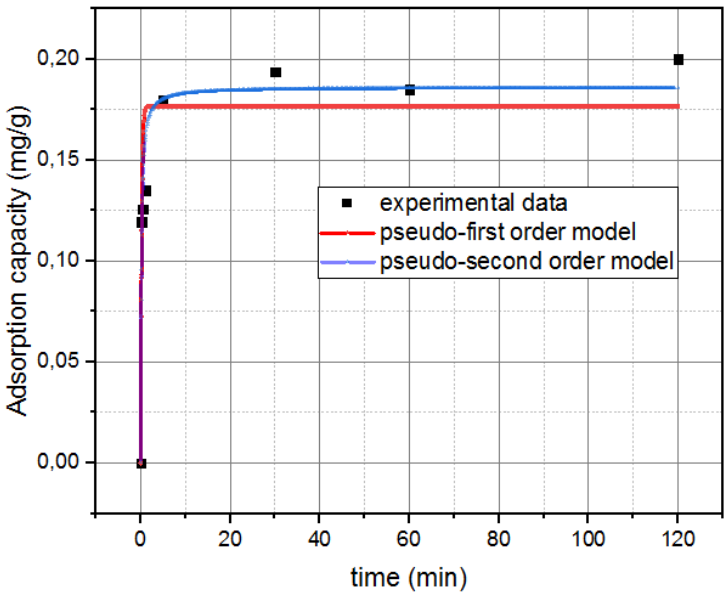

Figure 47: Kinetic model for ammonia initial concentration of 49 mg/l.

First of all is possible to see from the graphs at different initial concentration a similar behaviour of the material, the respond of the carbon nanotubes is almost immediate, in the first 30 seconds of contact the maximum value of adsorption capacity is almost reached.

For higher contact time the adsorption capacity remains constant unless some fluctuation due to experimental uncertainty, this brings to think that the contact time has not a great influence in the mechanism and adsorption occurs nearly instantaneously in the active site.

In the table 5. are reported the parameters obtained from the application of the models.

Initial concentration	Pseudo-first order model			Pseudo-second order model		
(mg/l)	Kf	qe	Adj. R-Square	Ks	qe	Adj. R-Square
33	7,60	0,179	0,9631	73,13	0,185	0,9917
49	4,40	0,177	0,8377	34,51	0,186	0,9326

Table 5: Kinetic parameter for different concentration of ammonia.

It is possible to notice that for both kinetic orders the value of the kinetics constant, kf for pseudo-first order model, ks for pseudo-second order model, decreases with increasing the initial concentration. This behaviour points out a difficult adsorption due to a higher value in the initial composition of ammonia. A lower value of kinetics constant could be related to a lower activation energy required, this could be related to the fact that when the concentration of ammonia in solution is bigger, more molecules are presents in the flow, so the probability to have a contact between the nanotube and the ammonia molecules increases.

The maximum adsorption capacity remains almost constant with the change in initial concentration, near 0,18 mg/g_{CNTs} for pseudo-first order and 0,19 mg/$_{CNTs}$ for pseudo-second order, this values are below the expectations compared with the adsorption capacity of other substances for which the adsorption capacity is at least one order of magnitude higher.

As the curve has just one change in slope, recalling the Weber-Morris model, probably only one mechanism concurs to the total adsorption. This mechanism of adsorption could be associated to a chemical adsorption instead of a physical-like one.

Anyway, all of the adsorption sites in the structure of CNTs suitable for ammonia are fulfilled and the adsorption process stops with the saturation of these active sites.

Comparing the statistical parameters obtained, it results evident that the pseudo-second order kinetic model has the best fit with respect to the experimental data.

Plazinski et al. associate the pseudo-second order kinetic model with intraparticle diffusion [36], it is possible to hypnotize that between ammonia molecules and Innovacarbon carbon nanotubes, intraparticle diffusion is exactly what happens.

The low adsorption values and the better fitting with the pseudo-second order let supposing the adsorption occurs at defect points of the graphitic structure.

Could be of great interest the analysis of the acetone used for regenerates the material, in order to check if the adsorbed ammonia can be released as happen with other substances, maybe due to stronger chemical bonds instead of weaker physical bonds the release of ammonia could results more difficult.

Kinetic model of adsorption for CNTs/solar oil system

The data of adsorption of solar oil with Innovacarbon material was fitted with pseudo-first order and pseudo-second order kinetic model. Also, in this case the general-order kinetic model does not converge with the experimental data.

Below are exposed the graphs representing the applied kinetics model to three different initial concentrations of solar oil in water.

The dots indicate the experimental points, the red line follow the trend of the pseudo-first order model while the blue one of the pseudo-second order model.

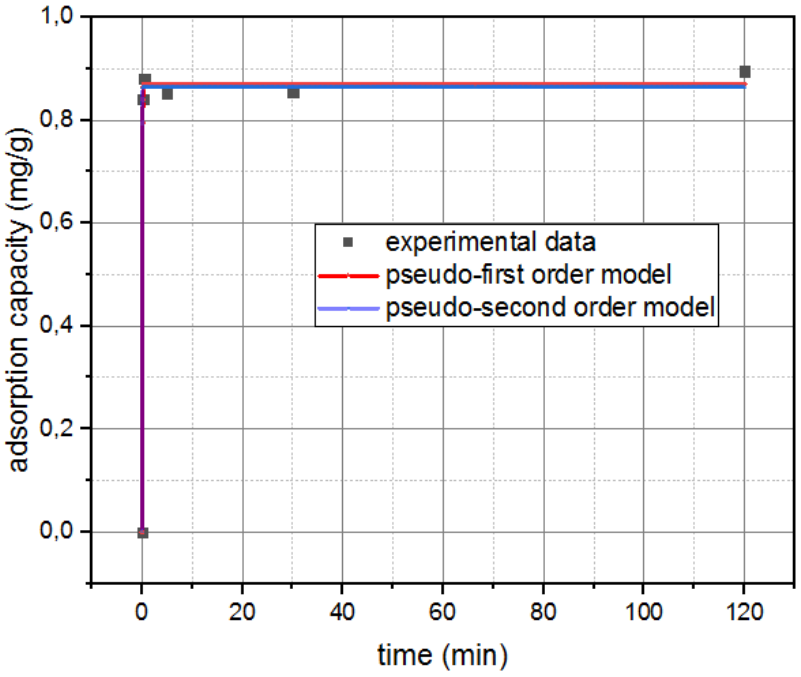

Figure 48: Kinetic model for solar oil with initial concentration of 45 mg/l.

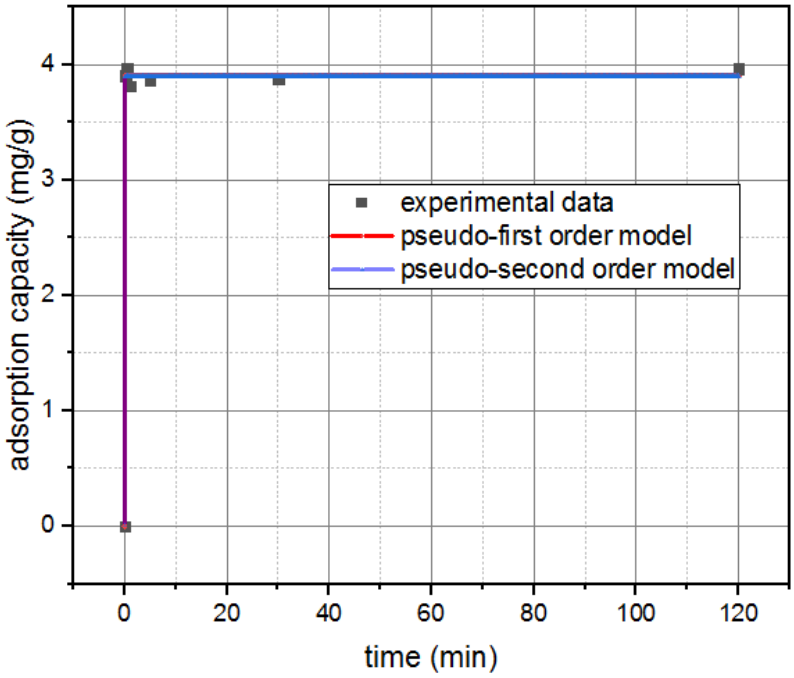

Figure 49: Kinetic model for solar oil with initial concentration of 204 mg/l.

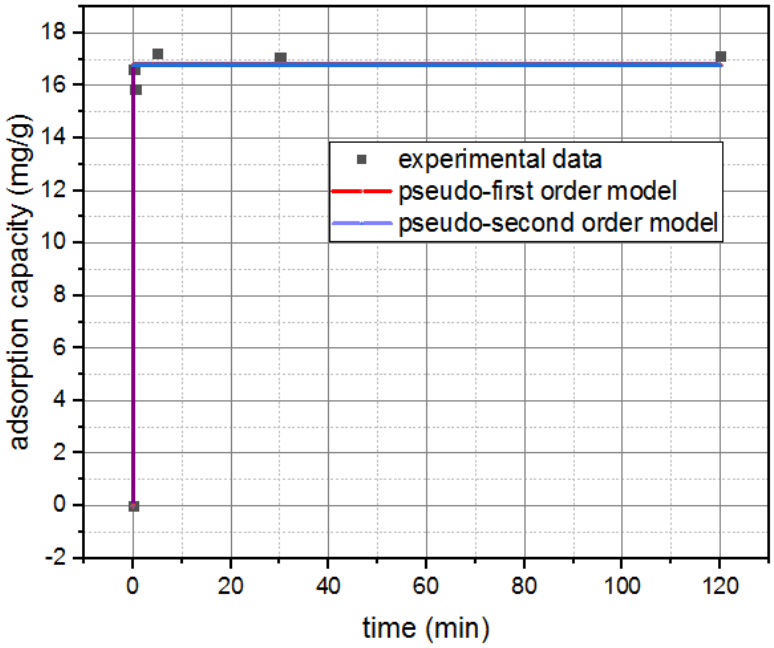

Figure 50: Kinetic model for solar oil with initial concentration of 878 mg/l.

The three graphs have a very similar shape, the curve relative to the pseudo-first order model perfectly overlap the curve of the pseudo-second order kinetic model, this is due to an adsorption practically instantaneous. The first experimental data at 10 s is already at a level of adsorption that is comparable to the maximum of adsorption for a specific initial concentration.

Furthermore, the shape of the graph suggests the presence of just one mechanism of adsorption, due to the absence of a sinusoidal form.

The solar oil is a mixture of substances highly hydrophobics, and the carbon nanotubes used are also highly hydrophobics and hydrophilic, so the interaction solar oil/CNTs is tremendous favoured by the similar nature of the analysed. This fact, together with short starting contact time due to the experimental setting leads to kinetic constant values very high, that can justify a great adsorption capacity of the nanotubes towards these organic molecules.

Van der Walls forces and π-π interaction probably play an important role in the as adsorption mechanism of solar oil by carbon nanotubes, as the molecules composing the solar oil recipe are principally of high molecular weight.

Initial concentration	pseudo-first order model			pseudo-second order model		
(mg/l)	Kf	qe	Adj. R-Square	Ks	qe	Adj. R-Square
45	20,35	0,870	0,9973	4,09E+44	0,864	0,9959
204	4350252,22	3,900	0,9983	4,28E+14	3,900	0,9983
878	5142462,94	16,781	0,9934	-2,03E+46	16,781	0,9934

Table 6: Kinetic parameter for different concentration of solar oil.

The values of Adj. R-square are very high and very similar between the two model, this maintains some uncertainty to stabilize which model better suits the data.

5.2 Isotherm model

The results obtained from the experiments permit to construct isothermal curve just for the interaction CNTs/solar oil. For the other substances, the obtained data does not permit this kind of modelling.

The experimental data has been interpolated with three isotherm models:

- Langmuir isotherm model
- Freundlich isotherm model
- Liu isotherm model

the graphs are presented in the figures below with the relative parameters in the table.

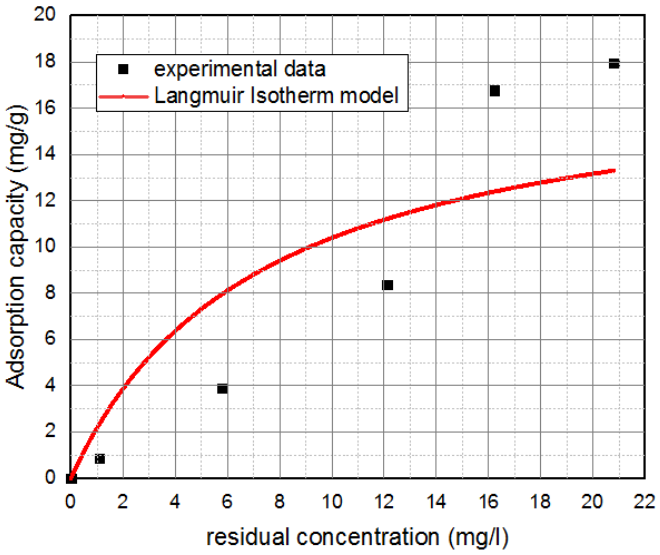

Figure 51: Langmuir isotherm model for CNTs/solar oil adsorption.

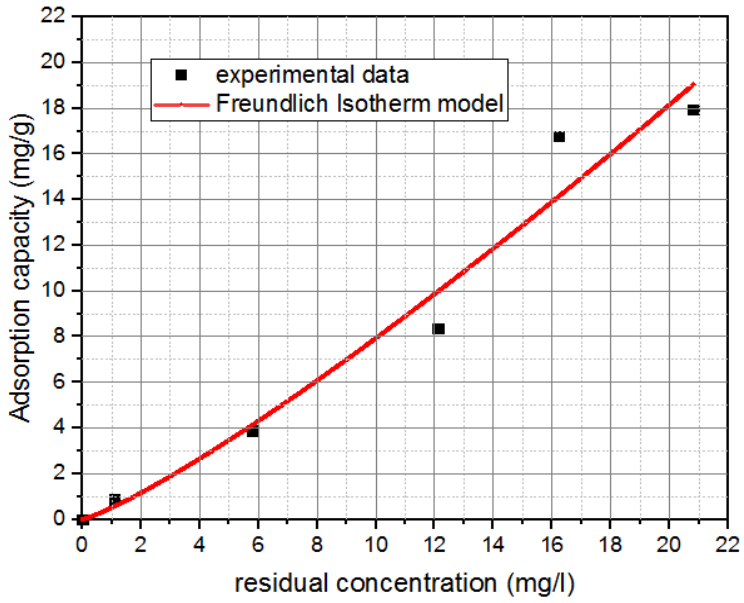

Figure 52: Freundlich isotherm model for CNTs/solar oil adsorption.

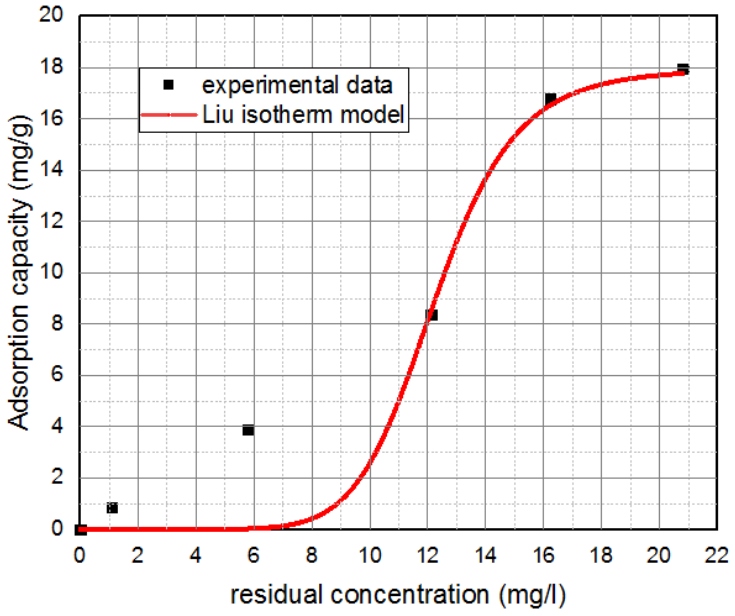

Figure 53: Liu isotherm model for CNTs/solar oil adsorption.

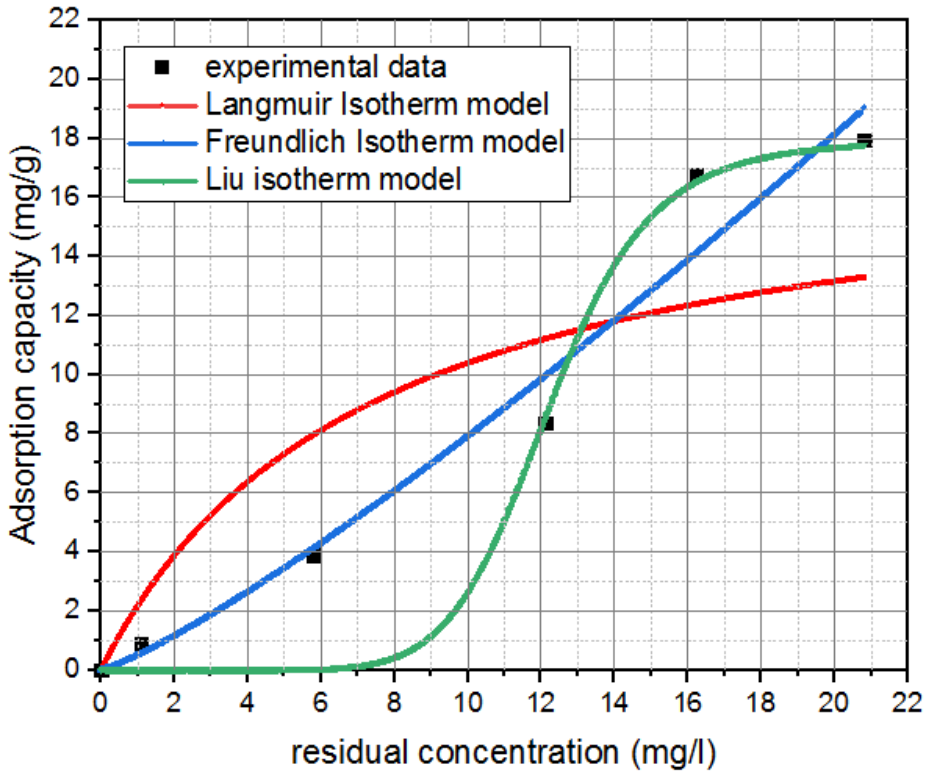

Figure 54: Comparison of CNTs/solar oil adsorption isotherms.

Langmuir isotherm model		Freundlich isotherm model			Liu isotherm model		
Kl	Adj. R-Square	Kf	n	Adj. R-Square	Kg	n	Adj. R-Square
0,14	0,7809	0,51	0,84	0,9560	3E-10	8,75	0,9355

Table 7: Isotherm model parameters.

Looking at the Adj. R-Square parameter for the three isotherm curve is possible to deduce that the model who better fit the experimental data is the Freundlich isotherm model, with an Adj. R-Square of 0,9560.

The Langmuir isotherm model fit very worst the data, this is probably due to the assumption of this model. Langmuir considers the formation of just a monolayer of the adsorbate over the surface of the adsorbent when it gets saturated. This is probably not true in the case of CNTs/solar oil interaction, in which it is more probable that a stratification of the adsorbate occurs as the adsorption process advances.

The Freundlich model has a great agreement of behaviour with the experimental data for low values of residual concentration, it is the only model that well

describes the first part of the graph. This behaviour let think it is due to the high hydrophobicity of both CNTs and solar oil. Firstly, there is almost immediately physical adsorption directly on the surface of carbon nanotubes, subsequently, other solar oil particles could remain trapped on other free available site of the CNTs or directly to the already adsorbed solar oil particle.

The Liu isotherm model fit very well the data for high values of residual concentration, because are discarded the assumption of monolayer adsorption of Langmuir isotherm model and infinite adsorption assumption of Freundlich isotherm model. For low values of residual concentrations, the model describes a too slow behaviour of adsorption who does not coincide with the obtained experimental points.

From the images below is possible to see the visible effect of the treatment, the oily appearance of the water is completely eliminated and also the perfume of chocolate and coco additives of the product is almost disappeared in the treated water, while before the treatment was intense and clearly the smell of chocolate and coco of the product.

Figure 55: 12 g of Solar oil in water and treated solution with Innovacarbon material.

During the desorption stage of the regeneration with acetone, the solar oil is released by CNTs and was clearly visible in the acetone, bringing to an oily yellow

turbidity appearance of the solution acetone/oil. It has been also possible to notice an increasing in the yellow coloration as was increased the initial concentration of the solution and so the adsorbed oil. For lower amounts of adsorbed oil, the solution acetone/oil appears of a whiter coloration.

 r

Figure 56: Acetone after regeneration of material used for adsorption of solar oil.

5.3 Maximum adsorption capacity

For extrapolate the values of maximum adsorption capacity of Innovacarbon material for the three analysed substances were used as reference the results obtained from the close circuit treatment experiments. Because, differently from the kinetic experiments, in this case the polluted solution passes more times through the material and more mechanism of adsorption could take place and considered.

The limit of adsorption and so the saturation of the filter is reached.

CNTs/Ammonia

From an initial concentration of ammonia of 25 mg/l, after four hours of close circuit system it has been possible to have a residual concentration of 15,85 mg/l for 250 ml of water treated with 150 g of material.

This leads to an adsorption capacity of 0,56 mg/g_{CNTs}. The results are shown in the graphs below.

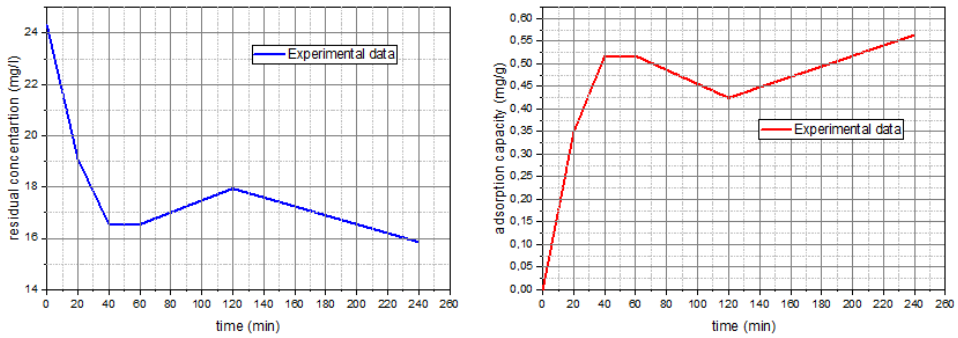

Figure 57: Residual concentration and adsorption capacity during treatment of ammonia solution with initial concentration of 25 mg/l.

If compared with the values find from the kinetic experiments (0,18-0,19 mg/g_{CNTs}), from the close circuit experiment results a bigger value of adsorption capacity (0,56 mg/g_{CNTs}), this could be consequence of the fact that, more than the contact time, a determinant factor could be how many times the particles could pass through the filter and so the possibility to encounter the adsorbent material and find some new available active site of adsorption.

This value is lower with respect to others encountered in literature, O. Moradi find a maximum adsorption capacity for CNTs/ammonia of around 9,20 mg/g_{CNTs} [32]. This could be related to a different characterization of carbon nanotubes, especially to a different functionalization.

As solution to improve the adsorption capacity could be the possibility to functionalize the carbon nanotubes with a more affine terminal group with ammonia, the negative consequence could be loss of hydrophobicity and the risk of leakage of material in water.

CNTs/Urea

For urea was compared the results obtained treating 250 ml of solution starting from two different concentration, 140 mg/l and 200 mg/l treated with 80 g of material.

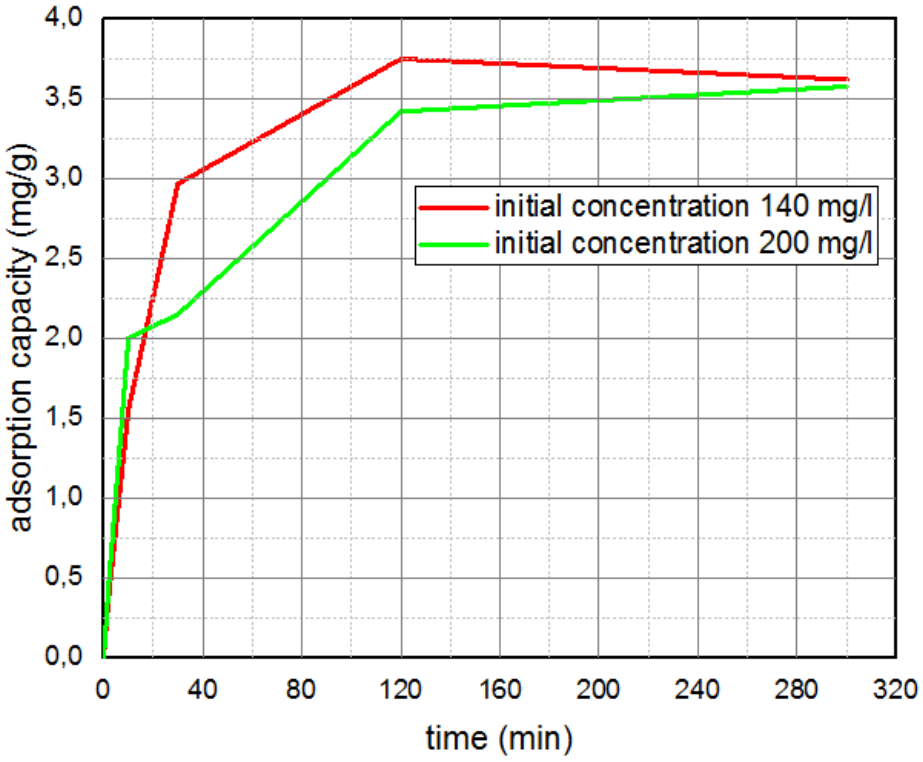

Figure 58: Adsorption capacity during treatment of urea solution with initial concentration of 140 mg/l (red line) and 200 mg/l (green line).

The graph shows a similar behaviour for the two concentration, with faster trend for short time when more urea is present in water, probably due to the fact that more particles encountered the material in the first minutes, for samples taken at higher times the behaviour tends to homogenize, reaching a similar adsorption capacity for the two cases. The adsorption capacity has been quantified to be 3,6 mg/g_{CNTs}.

This result as for ammonia is under the expectation, it is just one order of magnitude greater than the result obtained with ammonia. Comparing the molar mass of ammonia and urea, the molecule of urea weight almost 3 times the one of ammonia, so from the collected data is possible to estimate that more or less the double of particle of urea are adsorbed with respect to ammonia. This is not a great difference, that could be also intrinsic of the experimental error, so, it is thinkable that the same mechanism of adsorption work for both substances, maybe the difference could be given by an easier way to get in contact with a bigger molecule (Urea).

CNTs/Solar oil

From the experiments provided to define the maximum adsorption capacity of Innovacarbon carbon nanotubes to adsorb solar oil, it has been possible to reject the assumption of infinite adsorption of Freundlich isotherm model. It has been verified that there is a saturation limit for the material. When this limit is approached, the material still adsorbs but contemporary releases already adsorbed particles of solar oil, probably due to stratification mechanism of adsorption. The more external adsorbed molecules are released having a low interaction with CNTs.

The stratification mechanism is also known as surface condensation, while the organic chemicals adsorb on the CNTs surfaces, multilayer adsorption might happen. In this process, the first couple of layers collaborate with the surface, while the molecules further to the first two layers interact with each other. [45]

It was also possible to observe this effect as the released molecules tend to aggregate in little droplets of green appearance that are visible in the treated water. When the water is retreated, these molecules disappears and others with the same aspect are released in the water from the bottom of the filter, making the idea of an adsorption/desorption phenomena even more possible.

Fluctuation around a mean value of maximum adsorption is evident in the graph below for high number of passages of the liquid in the filter.

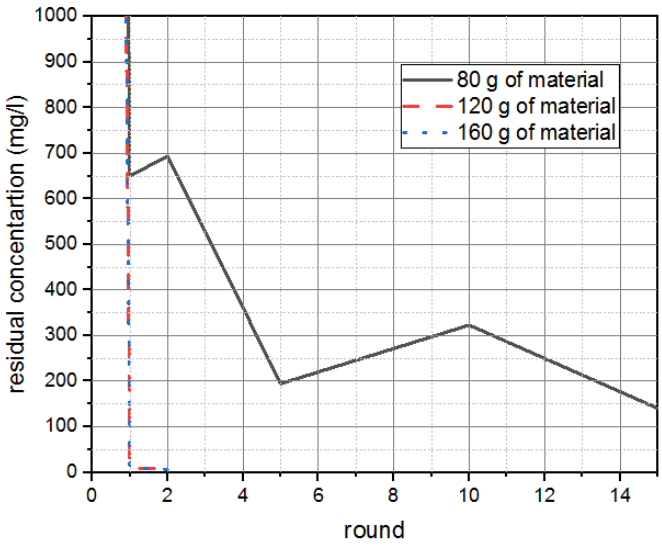

Figure 59: Residual concentration after treatment with 80g, 120g, 160g of material.

From the graph is possible to appreciate that for 120 g (red dot line) and 160 g (blue dot line) of material used, a solution with around 12 g/l of solar oil is practically totally purified after two round in the filter material, with a residual concentration of 6 mg/l that could be also less with instruments of analysis with more precision.

While using just 80 g (black line) of material is not been possible to eliminate all the 6 g of solar oil dispersed in water, an increase and decrease of the residual concentration is also observable, justifying the theorization of an adsorption/desorption mechanism derived from stratification.

Anyway, the saturation of the material has been reached and a maximum adsorption capacity of around 2500 mg/g_{CNTs} has been calculated. This means that each gram of CNTs can adsorb nearly 2,5 times its weight in solar oil particles. This value is ten thousands the limit reached for ammonia and urea, and it is comparable with the maximum adsorption capacity of Innovacarbon nanotubes for other substances such aromatics compounds, polyphenols, hydrocarbons and in general organic compounds. Substances that have a nature more similar to that presents in the solar oil.

Conclusions

Innovacarbon material has demonstrated adsorption properties that are not encountered in conventional adsorption materials for a very broad class of molecules.

The capacity of adsorbs oily substances is sensational and could add a great value to traditional sand filters. Although the results obtained with ammonia and urea are not at all satisfactory, but for very little concentration as that present in swimming pool of these contaminants, the material could contribute to eliminate these pollutants from the water, with a right sizing of the filter.

It is then possible to affirm that a filter with carbon nanotubes could improve the performance of the traditional sand filters, the analysis could pass then on the cost/benefits table.

The counter indication is related to the current price of CNTs, which exceeds that of other adsorbents such as powdered activated carbon (AC). Thus, a continuous massive production may eventually result in economies of scale in which the material may be produced economically for future large-scale applications.

Eventually, to reduce the cost of the filter but gain the benefits of carbon nanotubes could be possible to think in a two component filter, with a mix of sand and Innovacarbon material. Another way to improve the performance of the material could be the use of a tiny grain size, it has been demonstrated for other application an improve in performance reducing the grain size, as the number of nanotubes per weight of sand increases. The problem could be related to the head losses decreasing the void size for the passage of water.

Further studies could be focused on the behaviour of Innovacarbon material in adsorption of viruses and bacteria, in literature are already present works that demonstrate the effectiveness of carbon nanotubes in that application. Another interesting application could be the direct adsorption of DBPs such as THMs and HAAs from water.

The final goal could be reducing as much as possible the use of chlorine in treatment of swimming pool water providing a clean and zero waste solution, as all the materials would be recovered.

List of figures

List of tables

Bibliography

[1] L. Yang, «Regulation, formation, exposure, and treatment of disinfection by-products (DBPs) in swimming pool waters: A critical review,» *Environment International,* p. 1039–1057, 2018.

[2] D. Liviac, «Genotoxicity of Water Concentrates from Recreational Pools after Various Disinfection Methods,» *ENVIRONMENTAL SCIENCE & TECHNOLOGY,* pp. 3527-3532, 2010.

[3] W. L. Bradford, «What Bathers Put into a Pool: A Critical Review of Body Fluids and a Body Fluid Analog,» *International Journal of Aquatic Research and Education,* pp. 168-181, 2014.

[4] T. L. Teo, «Chemical contaminants in swimming pools: Occurrence, implications,» *Environment International,* pp. 16-31, 2015.

[5] C. Villanueva, «Bladder cancer and exposure to water disinfection by-products through ingestion, bathing, showering, and swimming in pools,» *American Journal of Epidemiology,* pp. 148-156, 2007.

[6] L. Tsamba, «+Chlorination by-products in indoor swimming pools: Development of a pilot pool unit and impact of operating parameters,» *Environment International 137,* 2020.

[7] M. Wood, «Role of filtration in managing the risk from Cryptosporidium in commercial swimming pools – a review,» *Journal of Water and Health,* pp. 357-370, 2019.

[8] PWTAG, «PWTAG code of practice,» 2019.

[9] J. Wyczarska-Kokot, «Impact of swimming pool water treatment system factors on the content of selected disinfection by-products,» *Environmental Monitoring and Assessment,* 2020.

[10] WHO, «Guidelines for safe recreational water environments,» WHO, 2006.

[11] EPA, «archive.epa.gov,» [Online]. Available: https://archive.epa.gov/enviro/html/icr/web/html/gloss_dbp.html.

[12] A. Bernard, «Chlorinated Pool Attendance, Atopy, and the Risk of Asthma during Childhood,» *Environmental Health Perspectives,* pp. 1567-1573, octuber 2006.

[13] J.-Q. J. Anna Cescon, «Filtration Process and Alternative Filter Media Material in Water Treatment,» *water,* p. 3377 , 2020.

[14] S. Iijima, «Helical microtubules of graphitic carbon.,» *Nature,* n. 354, pp. 56-58, 07 november 1991.

[15] M. Monthioux e V. Kuznetsov, «Who should be given the credit for the discovery of carbon nanotubes?,» *Carbon,* vol. 44, pp. 1621-1623, 01 august 2006.

[16] H. Golnabi, «Carbon nanotube research developments in terms of published papers and patents, synthesis and production,» *Scientia Iranica,* pp. 2012-2022, 2012.

[17] P. L.-B. Annick Loiseau, Understanding Carbon Nanotubes, Springer-Verlag Berlin Heidelberg, 2006.

[18] B. A. T. Khurshed A. Shah, «Synthesis of carbon nanotubes by catalytic chemical vapour deposition: A review on carbon sources, catalysts and substrates,» *Materials Science in Semiconductor Processing,* vol. 41, pp. 67-82, 2016.

[19] J. Han, «Structures and Properties of Carbon Nanotubes,» in *CarbonNanotubes science and applications*, 2004, pp. 1-24.

[20] J. Nakanishi, «Risk Assessment of the Carbon Nanotube Group,» *Risk Analysis,* vol. 35, n. 10, pp. 1940-1956, 2015.

[21] V. N. Popov, «Carbon nanotubes: properties and application,» *Materials Science and Engineering R 43,* p. 61–102, 2004.

[22] J. W. Mintmire, «ELECTRONIC AND STRUCTURAL PROPERTIES OF CARBON NANOTUBES,» pp. 37-46, 1995.

[23] C. Lu, «Adsorption of trihalomethanes from water with carbon nanotubes,» *Water Research 39,* p. 1183–1189, 2005.

[24] Z. Yu, *Synthesis of Carbon Nanofibers and Carbon Nanotubes,* 2005.

[25] J. Chrzanowska, «Synthesis of carbon nanotubes by the laser ablation method: Effect of laser wavelength,» *Phys. Status Solidi B,* vol. 252, n. 8, pp. 1860-1867, 2015.

[26] A. Yahyazadeh, «Carbon nanotube synthesis via the catalytic chemical vapor deposition of methane in the presence of iron, molybdenum, and iron–molybdenum alloy thin layer catalysts,» *Results in Physics 7,* p. 3826–3837, 2017.

[27] A. Policicchio, «Study of MWCNTs adsorption performances in gas processes,» *Journal of CO2 Utilization,* pp. 30-39, 2015 .

[28] R. Das, «Can We Optimize Arc Discharge and Laser Ablation for Well-Controlled Carbon Nanotube Synthesis?,» *Nanoscale Research Letters,* pp. 1-23, 2016.

[29] F. M. Machado, «Carbon Nanoadsorbents,» in *Carbon Nanomaterials as Adsorbents for Environmental and Biological Applications*, springer, 2015, pp. 11-32.

[30] É. C. Lima, «Kinetic and Equilibrium Models,» in *Carbon Nanomaterials as Adsorbents for Environmental and Biological Applications*, 2015, pp. 36-37.

[31] G. Ersan, «Adsorption kinetics and aggregation for three classes of carbonaceous adsorbents in the presence of natural organic matter,» *Chemosphere,* n. 229, pp. 512-524, 2019.

[32] O. Moradi, «Applicability comparison of different models for ammonium ion adsorption by multi-walled carbon nanotube,» *Arabian Journal of Chemistry (2016),* p. S1170–S1176, 2011.

[33] A. Dąbrowski, «Adsorption — from theory to practice,» *Advances in Colloid and Interface Science,* vol. 93, pp. 135-224, 2001.

[34] E. C. D. Djebbar Tiab, «Shale-Gas Reservoirs,» in *Petrophysics (Fourth Edition)*, Gulf Professional Publishing, 2016, pp. 719-774.

[35] J.-D. R. Rocha, «Emerging investigators series: highly effective adsorption of organic aromatic molecules from aqueous environments by electronically sorted single-walled carbon nanotubes,» *Environmental Science Water Research & Technology,* pp. 203-212, 2017.

[36] W. Plazinski, «Modeling of sorption kinetics: the pseudo-second order equation and the sorbate intraparticle diffusivity,» *Adsorption ,* p. 1055–1064, 2013 .

[37] A. Peigney, «Specific surface area of carbon nanotubes and bundles of carbon nanotubes,» *Carbon 39,* pp. 507-514, 2001 .

[38] S. Kurwadkar, «Application of carbon nanotubes for removal of emerging contaminants of concern in engineered water and wastewater treatment systems,» *Nanotechnology for Environmental Engineering,* pp. 4-12, 2019.

[39] S. Kurwadkar, «Application of carbon nanotubes for removal of emerging contaminants of concern in engineered water and wastewater treatment systems,» *Nanotechnology for Environmental Engineering,* pp. 4-12, 2019.

[40] K. Zare, «A comparative study on the basis of adsorption capacity between CNTs and activated carbon as adsorbents for removal of noxious synthetic dyes: a review,» *J Nanostruct Chem,* vol. 5, p. 227–236, 2015.

[41] T. Liu, «Oil Adsorption and Reuse Performance of Multi-Walled Carbon Nanotubes,» *Procedia Engineering,* n. 102, p. 1896 – 1902, 2015.

[42] K. Pyrzynska, «Carbon Nanotubes as a New Solid-Phase Extraction Material for Removal and Enrichment of Organic Pollutants in Water,» *Separation & Purification Reviews,* pp. 372-389, 2008.

[43] B. Pan e B. Xing, «Adsorption Mechanisms of Organic Chemicals on Carbon Nanotubes,» *ENVIRONMENTAL SCIENCE & TECHNOLOGY,* pp. 9005-9013, 2008.

[44] M. Šolic', «Comparing the Adsorption Performance of Multiwalled Carbon Nanotubes Oxidized by Varying Degrees for Removal of Low Levels of Copper, Nickel and Chromium(VI) from Aqueous Solutions,» *water,* 2020.

[45] T. A. Abdullah, «Functionalized multi-walled carbon nanotubes for oil spill cleanup from water,» 2021.

[46] B. Verma, «Synthesis of carbon nanotubes via chemical vapor deposition: an advanced application in the Management of Electroplating Effluent,» *Environmental Science and Pollution Research,* p. 14007–14018, 2020.